Title
β-Lactones: A Novel Class of Ca2+-Independent Phospholipase A2 (Group VIA iPLA2) Inhibitors with the Ability To Inhibit β-Cell Apoptosis

Journal
Journal of Medicinal Chemistry, 62(6)

ISSN
0022-2623

Authors
Dedaki, Christina
Kokotou, Maroula G
Mouchlis, Varnavas D
et al.

Publication Date
2019-03-28

DOI
10.1021/acs.jmedchem.8b01216

Peer reviewed

J Med Chem. Author manuscript; available in PMC 2020 March 28.

Published in final edited form as:

J Med Chem. 2019 March 28; 62(6): 2916–2927. doi:10.1021/acs.jmedchem.8b01216.

β-Lactones: A Novel Class of Ca^{2+}-Independent Phospholipase A_2 (Group VIA iPLA$_2$) Inhibitors with Ability to Inhibit β-Cell Apoptosis

Christina Dedaki[†], **Maroula G. Kokotou**[†,§], **Varnavas D. Mouchlis**[§], **Dimitris Limnios**[†,§], **Xiaoyong Lei**[#,‡], **Carol T. Mu**[§], **Sasanka Ramanadham**[#,‡], **Victoria Magrioti**[*,†], **Edward A. Dennis**[*,§], **George Kokotos**[*,†]

[†]Laboratory of Organic Chemistry, Department of Chemistry, National and Kapodistrian University of Athens, Panepistimiopolis, Athens 15771, Greece

[§]Department of Chemistry and Biochemistry and Department of Pharmacology, School of Medicine, University of California, San Diego, La Jolla, California 92093-0601, USA

[#]Department of Cell, Developmental and Integrative Biology, University of Alabama at Birmingham, Birmingham, AL 35294, USA

[‡]Comprehensive Diabetes Center, University of Alabama at Birmingham, Birmingham, AL 35294, USA

Abstract

Interest in Ca^{2+}-independent phospholipase A_2 (GVIA iPLA$_2$) has accelerated recently as it is being recognized as a participant in biological processes underlying diabetes development and autoimmune-based neurological disorders. The development of potent GVIA iPLA$_2$ inhibitors is of great importance, because only a few have been reported so far. We present a novel class of GVIA iPLA$_2$ inhibitors based on the β-lactone ring. This functionality in combination with a four-carbon chain carrying a phenyl group at position-3, and a linear propyl group at position-4 of the lactone ring confers excellent potency. *trans*−3-(4-Phenylbutyl)-4-propyloxetan-2-one (GK563) was identified as being the most potent GVIA iPLA$_2$ inhibitor ever reported (X_I(50) 0.0000021, IC_{50} 1 nM) and also one that is 22,000 times more active against GVIA iPLA$_2$ than GIVA cPLA$_2$. It was found to reduce β-cell apoptosis induced by pro-inflammatory cytokines, raising the possibility that it can be beneficial in countering autoimmune diseases, such as type 1 diabetes.

Graphical Abstract

[*]**Corresponding Author** For G.K.: phone: +30 210 7274462; fax: +30 210 7274761; gkokotos@chem.uoa.gr., For E.A.D.: phone: +1 858 534 3055; edennis@ucsd.edu. For V.M.: phone: +30 210 7274497; vmagriot@chem.uoa.gr.

Associated Content

Supporting Information.

Code numbers of tested compounds, elemental analyses of synthesized compounds, XP GScores for the all the diastereomers of **9k**, chromatographs of **9k**, *trans*-**9k** and *cis*-**9k**, NMR spectra of *trans*-**9k** and *cis*-**9k**. (PDF)

Molecular formula strings and inhibition data (CSV)

This material is available free of charge via the Internet at http://pubs.acs.org.

Keywords

β-cell apoptosis; β-lactones; Ca^{2+}-independent phospholipase A_2; cytosolic phospholipase A_2; inhibitors

INTRODUCTION

The phospholipase A_2 (PLA_2) superfamily consists of diverse enzymes, which are currently categorized into sixteen groups and many subgroups and all are able to hydrolyze the ester bond at the *sn*-2 position of glycerophospholipids.[1] A number of these enzymes do not require Ca^{2+} ions either for their activity or for the translocation to membranes and are classified as Ca^{2+}-independent PLA_2s.[1–5] The initial reports of Ca^{2+}-independent PLA_2 activity referred to a 40-kDa enzyme described as $iPLA_2$.[6,7] Subsequently, an 85-kDa $iPLA_2$ was purified and characterized from macrophages[8] and cloned from hamster, mouse, and rat[9–11] and is now designated as Group VIA (GVIA) $iPLA_2$ (also $iPLA_2\beta$). To date, the group VI Ca^{2+}-independent PLA_2 includes six different subgroups: GVIA ($iPLA_2\beta$), GVIB ($iPLA_2\gamma$), GVIC ($iPLA_2\delta$), GVID ($iPLA_2\varepsilon$), GVIE ($iPLA_2\zeta$), and GVIF ($iPLA_2\eta$).[1] Among them, GVIA is the most well studied and recognized $iPLA_2$. The human GVIA $iPLA_2$ (806 amino acids) contains seven ankyrin repeats (residues 152–382), a linker region (residues 383–474) with the eighth repeat disrupted by a 54-amino-acid insert, and a catalytic domain (residues 475–806). The active site serine of GVIA $iPLA_2$ lies within a lipase consensus sequence (Gly486-X-Ser519-X-Gly487) in the catalytic domain. Although GVIA $iPLA_2$ and the other major intracellular PLA_2, the calcium-dependent GIVA $cPLA_2$, both use a serine/aspartate catalytic dyad for their catalytic mechanism, GVIA $iPLA_2$ does not show arachidonic acid-selectivity while GIVA $cPLA_2$ does.[12]

PLA_2s have been implicated in a number of physiological and pathophysiological processes. Thus, a variety of synthetic inhibitors have been generated and studied *in vitro*, as well as *in vivo*.[1,13–15] The majority of these inhibitors have been developed to target cytosolic GIVA $cPLA_2$[16] and secreted $sPLA_2$.[17] Inhibitors of GVIA $iPLA_2$ had attracted less interest, because the enzyme's role was less well understood. The first introduced inhibitor for $iPLA_2$ was a bromoenol lactone compound (**1**, BEL,[18] Figure 1) which is an irreversible, covalent inhibitor of GVIA $iPLA_2$.[18] It has been used widely to delineate the specific role of GVIA $iPLA_2$ in variety of systems and biological processes.[1,13] Although BEL is selective against GVIA $iPLA_2$ versus other PLA_2s, it also inhibits other serine enzymes (i.e. magnesium-dependent phosphatidate phosphohydrolase)[19] and therefore the data obtained from *ex vivo* and *in vivo* studies of its inhibitory activity must be carefully considered.

The GVIA $iPLA_2$ is involved in lipid signaling and pathological conditions including diabetes,[4,5,20] Barth syndrome[21] and progesterone-induced acrosome exocytosis.[22] The recent emergence of GVIA $iPLA_2$ as a contributor to pathophysiology prompted us to explore the possibility that more potent and selective GVIA $iPLA_2$ inhibitors can be developed.

In our first series of chemical synthesis, we generated polyfluoroketone-based compounds that proved to be more potent and selective than BEL, with the added feature of manifesting reversible inhibition of GVIA $iPLA_2$. These compounds contained an aromatic ring and a small aliphatic chain as a spacer between the two functional groups.[23–25] One of these first generation fluoroketones, FKGK11[23] (**2a**, Figure 1, $X_I(50)$ 0.0014[24]), was used *in vivo* to demonstrate a role for GVIA $iPLA_2$ in both the onset and progression of experimental autoimmune encephalomyelitis, an animal model of multiple sclerosis.[26] Further, the combination of BEL or FKGK11 with anticancer drug paclitaxel was highly effective in blocking ovarian cancer development.[27]

Subsequent structure-activity relationship studies with the polyfluoroketones led to the generation of FKGK18[24] (**3**, Figure 1, $X_I(50)$ 0.0002[24]), which contained a naphthyl ring and a trifluoromethyl group instead of a phenyl ring and a pentafluoroethyl group, respectively. FKGK18 was found to be 195 and >455 times more potent for GVIA $iPLA_2$ than for GIVA $cPLA_2$ and GV $sPLA_2$, respectively. In view of this, FKGK18 was deemed a valuable tool to explore the role of GVIA $iPLA_2$ in cells and *in vivo* models. Those studies revealed that FKGK18 was able to inhibit β-cell apoptosis[28] and that its administration to spontaneous diabetes-prone non obese diabetic (NOD) mice significantly reduced diabetes incidence in association with reduced insulitis, improved glucose homeostasis, higher circulating insulin and β-cell preservation.[20] Subsequently, GK187[25] a more potent and selective GVIA $iPLA_2$ inhibitor (**2b**, Figure 1, $X_I(50)$ 0.0001[25]) was identified. To gain a greater understanding of the enzyme-inhibitor interactions, a robust homology model was developed based on hydrogen/deuterium exchange mass specrtometry experimental data and molecular dynamics simulations.[29–31] Combining this with computational chemistry, organic synthesis and *in vitro* assays led to identification of new thioether fluoroketone inhibitors as well as a novel thioether keto-1,2,4-oxadiazole inhibitor (**4**, Figure 1, $X_I(50)$ 0.0057) of GVIA $iPLA_2$.[32]

The need for more potent and selective inhibitors of GVIA $iPLA_2$ and the potential pharmacological limitations of fluoroketones as human therapeutics, led us to the quest of additional functional series of inhibitors. In this work, we developed a novel class of GVIA $iPLA_2$ inhibitors based on a β-lactone ring. The design and the synthesis of a variety of these inhibitors, as well as assessment of their selectivity towards the three main human PLA_2s are reported. Furthermore, the ability to reduce β-cell apoptosis induced by pro-inflammatory cytokines is demonstrated.

RESULTS AND DISCUSSION

Design and synthesis of inhibitors.

Lipstatin (**5a**, Figure 2), a natural product isolated from *Streptomyces toxytricini*, is a potent inhibitor of pancreatic lipase[33] and the semisynthetic derivative tetrahydrolipstatin (Orlistat, **5b**, Figure 2) is an approved drug for the treatment of obesity inhibiting lipase and thus preventing the absorption of fats from the human diet. Studies on the mode of action of tetrahydrolipstatin revealed that an enzyme-inhibitor complex of an acyl-enzyme type is formed, which slowly decomposes, and that the β-lactone ring is the functional group of tetrahydrolipstatin reacting with the active site of the enzyme.[34] Several other natural products containing a β-lactone ring are enzyme inhibitors and present attractive pharmacological properties, for example marizomib (**6**, Figure 2) is a proteasome inhibitor recently approved as an orphan drug by FDA for the treatment of multiple myeloma.[35] Structural modifications of naturally occurring β-lactones have been proposed as an effective strategy for generating new drugs for treating bacterial infections, cancer, obesity and hyperlipidemia.[36]

In general, the strained β-lactone ring is expected to be attacked by the hydroxyl group of the active site serine of a serine-hydrolase. GVIA $iPLA_2$ utilizes a serine residue in its catalytic mechanism, thus, in principle it may interact with a β-lactone ring. Our previous studies on GVIA $iPLA_2$ inhibitors have shown that a potential inhibitor has to be a small non-polar molecule.[23–25] In addition, an aromatic ring attached to a four-carbon chain seems to fit very well into the binding site of GVIA $iPLA_2$. Thus, we designed a β-lactone and chose one of the substituents to be a medium carbon chain carrying an aromatic ring in varying distances (Ar-Cn) from the lactone ring. The second substituent is a small aliphatic chain (-R) containing one to six carbon atoms. The general structure of the lactones we designed is depicted in Figure 2.

The general route for the synthesis of the designed β-lactones is depicted in Scheme 1. A variety of carboxylic acids containing an aromatic group at the end of the chain were chosen as starting materials. Carboxylic acids **7a-f** were deprotonated by treatment with LDA and after reaction with commercially available aliphatic aldehydes RCHO,[37] β-hydroxy acids **8a-k** were obtained. Finally, cyclization of the intermediate α,β-substituted β-hydroxy acids **8a-k** upon treatment with p-toluenesulfonyl chloride[38] led to α,β-substituted β-lactones **9a-k** (Scheme 1).

Both β-hydroxy acids **8a-k** and β-lactones **9a-k** were obtained as mixtures of diastereomers, whose ratio was estimated by ^{1}H NMR spectroscopy. For β-hydroxy acids **8a-k**, the ratio of the peak integrations corresponding to methinic C*H*OH signals was used to estimate the ratio of *anti*:*syn* diastereomers and varied from 7:3 to 6:4. For β-lactones, the ratio of the peak integrations corresponding to methinic proton of either C-3 or C-4 indicated a ratio of *trans*:*cis* diastereomers varying from 9:1 to 7:3. *trans* β-Lactones were obtained in excess being thermodynamically more stable than their counterparts *cis* products, and their geometry was determined by ^{1}H NMR based on the chemical shifts reported in literature for similar compounds. In accordance to literature data, characteristic peaks for 3-CH and 4-CH are reported at 3.2 and 4.2 ppm, respectively, for *trans* β-lactones,[39] while the corresponding chemical shifts for *cis* β-lactones are reported at 3.6 and 4.5 ppm, respectively.[40] The *trans* and *cis* diastereomers of **9d, e, f, j** and **k** were separated by column chromatography. In particular for **9k**, the coupling constants between the C-3 and C-4 protons were measured to be 4.0 Hz and 6.7 Hz for the *trans* and the *cis* diastereomer (see, Supporting Information), respectively, values which are in accordance with those reported in the literature.[40] Further, in ^{13}C NMR spectra, the chemical shifts corresponding to C-3 and C-4 are at 56.0 ppm and

77.9 ppm for the *trans* diastereomer, while at 52.6 ppm and 75.4 ppm for the *cis* diastereomer.

In vitro inhibition of GVIA iPLA$_2$, GIVA cPLA$_2$ and GV sPLA$_2$.

All synthesized β-lactones were tested for their *in vitro* inhibitory activity on recombinant human GVIA iPLA$_2$ using mixed micelle assays. In addition, their selectivity over human GIVA cPLA$_2$ and GV sPLA$_2$ was also studied using similar group-specific mixed micelle assays. The initial screening assays for the *in vitro* inhibition of human GVIA iPLA$_2$, GIVA cPLA$_2$ and GV sPLA$_2$ for the racemic lactones and their comparison with previously reported fluroketones and oxadiazoles inhibitors were carried out using our previously described radioactivity-based mixed micelle assay.[41–43] For the most potent lactones, the *trans* and *cis* diastereomers were prepared and our previously described lipidomics-based mixed micelle assay was employed to determine their activities.[44,45] The inhibition results presented in Table 1 are either as percent inhibition or as $X_I(50)$ values. At first, the percent of inhibition for each PLA$_2$ enzyme at 0.091 mole fraction of each inhibitor was determined. Then, the $X_I(50)$ values were measured for compounds that displayed greater than 95% inhibition of GVIA iPLA$_2$. The $X_I(50)$ is the mole fraction of the inhibitor in the total substrate interface required to inhibit the enzyme activity by 50%. Data for inhibitors **2a**,[24] **2b**,[25] **3**[24] and **4**[32] (tested under the same radioactivity-based assay conditions) are included in Table 1 for comparison purposes.

The curves for the concentration dependence of the inhibition of GVIA iPLA$_2$ by β-lactones were fit to sigmoidal curves and those of *trans*-**9k** (GK563) and *cis*-**9k** (GK564) are presented as examples in Figure 3.

At first, β-lactones carrying an aromatic group at the end of a three-carbon atom chain and an n-hexyl chain as substituents (compounds **9a**, **9b** and **9c**) were tested. Irrespective of the nature of the aromatic group (phenyl, naphthyl, biphenyl), none of these presented significant inhibition (< 90%) of GVIA iPLA$_2$ (entries 1–3). However, it seemed that a simple phenyl (**9a**), instead of a naphthyl (**9c**) or a biphenyl (**9b**), group led to greater inhibition. Then, the hexyl chain was reduced to a shorter chain of three-carbon atoms. Interestingly, all three compounds (**9d**, **9e** and **9f**) combining an aromatic group at the end of a three-carbon atom chain and a n-propyl chain (entries 4, 7 and 10) presented significant inhibition (96–98%) of GVIA iPLA$_2$. The mixtures of these compounds were separated by column chromatography and the potencies of the corresponding *trans* and *cis* diastereomers were evaluated. Both *trans*-**9d** and *cis*-**9d** presented significant inhibition for both GVIA iPLA$_2$ and GIVA cPLA$_2$ (entries 5 and 6). However, *trans*-**9d** seemed to be more potent inhibitor of GVIA iPLA$_2$ with an $X_I(50)$ value of 0.00019 (IC$_{50}$ 95 nM, entry 5), while *cis*-**9d** more potent for GIVA cPLA$_2$ with an $X_I(50)$ value of 0.0019 (IC$_{50}$ 0.95 μM, entry 6). Among the naphthyl derivatives *trans*-**9e** and *cis*-**9e** (entries 8 and 9), *trans*-**9e** was found more potent inhibiting GVIA iPLA$_2$ with an $X_I(50)$ value of 0.00030 (IC$_{50}$ 0.15 μM, entry 8). For the para-methoxyphenyl derivatives *trans*-**9f** and *cis*-**9f** (entries 11 and 12), an interesting selectivity seems to take shape. *trans*-**9f** inhibited GVIA iPLA$_2$ with an $X_I(50)$ value equal to that estimated for *trans*-**9d** (0.00019, IC$_{50}$ 95 nM, entry 11). However, *cis*-**9f** proved to be a potent inhibitor of GIVA cPLA$_2$ ($X_I(50)$ 0.00004, IC$_{50}$ 20 nM, entry 12) being almost 1000 times more potent for GIVA $cPLA_2$ than for GVIA $iPLA_2$ ($X_I(50)$ 0.038, IC_{50} 20 μM, entry 12).

When the linear n-propyl group of **9d** was replaced by a branched isopropyl group (compound **9g**, entry 13), the inhibitory potency over GVIA $iPLA_2$ was reduced. Replacement of the n-propyl group of **9e** by an ethyl or a methyl group (compounds **9h**, **9i**, entries 14 and 15) resulted in a reduction of the inhibitory potency. Clearly, a small linear chain of three-carbon atoms led to superior inhibitory results over GVIA $iPLA_2$ in comparison to a medium chain of six-carbon atoms or a short chain of one or two carbon atoms.

Thus, by keeping a linear three-carbon chain at position-4, the distance between the aromatic group and the lactone ring at position-3 was increased by one carbon atom resulting in compounds **9j** and **9k**, which both presented high inhibition of GVIA $iPLA_2$ (97–100%, entries 16 and 19). The diastereomers were separated by column chromatography and the potencies of both *trans* and *cis* diastereomers of **9j** and **9k** were estimated. Both the naphthyl derivatives *trans*-**9j** and *cis*-**9j** were found to inhibit GVIA $iPLA_2$ with $X_I(50)$ values of 0.00009 (IC_{50} 45 nM, entry17) and 0.0021 (IC_{50} 1 μM, entry 18), respectively, but did not present significant inhibition of GIVA $cPLA_2$ (59% and 72% at a high concentration of 0.091 mole fraction, respectively, entries 17 and 18). Gratifyingly, the combination of a four-carbon chain carrying a phenyl group at position-3 and a linear propyl group at position-4 of the lactone ring led to the best results. The *trans* diastereomer of **9k** [*trans*-(±)-3-(4-phenylbutyl)-4-propyloxetan-2-one, GK563] was found to be a highly potent inhibitor of GVIA $iPLA_2$ with a $X_I(50)$ value of 0.0000021 (IC_{50} 1 nM, entry 20), while the *cis* diastereomer of **9k** [*cis*-(±)-3-(4-phenylbutyl)-4-propyloxetan-2-one, GK564] was a dramatically weaker inhibitor, presenting a $X_I(50)$ value of 0.007 (IC_{50} 3.5 μM, entry 21). Both *trans*-**9k** and *cis*-**9k** were found to be weaker inhibitors of GIVA $cPLA_2$. In particular for inhibitor *trans*-**9k**, its $X_I(50)$ value for GIVA $cPLA_2$ was measured to be 0.042 (IC_{50} 22 μM) indicating 22,000 times selectivity.

None of the β-lactones presented any appreciable inhibition of GV $sPLA_2$. The percentage inhibition of GV $sPLA_2$ did not exceed 47% (entry 1) at a high concentration of 0.091 mole fraction.

The results of *in vitro* inhibition clearly confirm our assumption that β-lactones inhibit the serine-based GVIA $iPLA_2$. However, a careful selection of the heterocyclic ring substituents is critical for potent inhibition. β-Lactone *trans*-**9k** stands out as the most potent inhibitor of GVIA $iPLA_2$ ever reported in literature, outperforming the potent fluoroketone FKGK18 ($X_I(50)$ value of 0.0002[24], IC_{50} 100 nM), which has been used successfully for *in vivo* studies.[20]

Binding mode and interactions of 9k diastereomers.

Lactones constitute a novel class of compounds identified as potent GVIA $iPLA_2$ inhibitors. The binding mode of the most active compound in the active site of the enzyme was determined in our effort to understand its interactions with critical residues of the active site. For the docking calculations, the previously published docked structures of GIVA $cPLA_2$

and GVIA $iPLA_2$ based on our molecular dynamics simulations with two different fluoroketone compounds in the active site were used.[31,32,44] An average theoretical score of 6.0 kcal/mol was calculated for all four diastereomers of the most potent lactone GVIA $iPLA_2$ inhibitor **9k** (Table S3, Supporting Information). The binding mode of *trans*-(*S*,*S*)-**9k** in the resulting optimized docked structure showed close proximity of the carbonyl group to the oxyanion hole (Gly486/Gly487) of GVIA $iPLA_2$, while the aromatic chain was placed in the hydrophobic area of the active site, interacting with residues such as Tyr541, Met544, Val548, Phe549, Tyr643, and Leu770. The small aliphatic tail of the inhibitor was located close to Ala640 and Pro641 (Figure 4B). The lactone inhibitor *trans*-(*S*,*S*)-**9k** exhibited lower inhibition towards GIVA $cPLA_2$. The binding mode in the active site of GVIA $cPLA_2$ also showed close proximity of the carbonyl group to the oxyanion hole (Gly197/Gly198) (Figure 4A). The aromatic chain was also located in the hydrophobic area of GVIA $cPLA_2$, but its small size does not complement the suitable aromatic interactions with the active site of GIVA $cPLA_2$.

Suppression of cytokine-induced β-cell apoptosis.

Type 1 diabetes (T1D) is a consequence of autoimmune destruction of islet β-cells. It is recognized that eicosanoids play important roles in promoting inflammatory responses in several diseased states, including diabetes.[46] We reported that inhibition of the GVIA $iPLA_2$ ($iPLA_2\beta$) mitigates β-cell death[47–52] raising the possibility that inhibitors of GVIA $iPLA_2$ may be beneficial in reducing β-cell death that leads to T1D incidence. To date, several inhibitors that can inhibit GVIA $iPLA_2$ are available, but they have limitations.[1,13–15] As we noted in introduction, recent efforts to generate more selective and potent GVIA $iPLA_2$ inhibitors identified reversible fluoroketone compounds as being selective towards GVIA.[23–25] One such inhibitor, designated FKGK18, was recently described to be more selective towards $iPLA_2\beta$ than $iPLA_2\gamma$ (GVIB $iPLA_2$).[28] Under *in vitro* conditions, FKGK18 inhibited insulin secretion and β-cell apoptosis.[28] Under *in vivo* conditions, it was devoid of cytotoxicity and effective in reducing T1D incidence.[20] Thus, novel GVIA $iPLA_2$ inhibitors are very attractive as candidates for preventing β-cell apoptosis and as potential new agents for preventing T1D development.

Here, we assessed the ability of *trans*-**9k** in reducing β-cell apoptosis by treating INS-1 cells with pro-inflammatory cytokines (IL-1β + IFNγ) in the absence and presence of *trans*-**9k**. As expected, cytokine exposure resulted in a dramatic increase in β-cell apoptosis (Fig. 5). At 0.10 μM and 1.0 μM, *trans*-**9k** alone had no effect, but it promoted a slight but modest rise in cell death. Co-treatment of the cells with cytokines and *trans*-**9k** produced a concentration-dependent inhibition of β-cell apoptosis; with 0.10 μM showing minimal and non-significant effect, but significant decreases evident with 1.0 μM (28%) and 10.0 μM (41%). In comparison, these results are similar to those seen with *S*-BEL,[47] a selective inhibitor of $iPLA_2\beta$. However, in contrast to *S*-BEL, continuous exposure of *trans*-**9k** to cells was not cytotoxic at 0.10 or 1.0 μM, and induced only a modest rise in percent cell death (DMSO, 7.06 ± 0.36 vs. *trans*-**9k**, 9.51 ± 0.78, $p = 0.012$) at 10 μM. These findings suggest that *trans*-**9k** is another candidate inhibitor of GVIA $iPLA_2$ suitable for further studies and raise the possibility that its use *in vivo* may be beneficial in reducing β-cell death leading to T1D.

CONCLUSION

Herein, we describe a novel class of GVIA $iPLA_2$ inhibitors based on the β-lactone ring. This reactive functionality in combination with a four-carbon chain carrying a phenyl group at position-3, and a linear propyl group at position-4 of the lactone ring produced the best candidate inhibitor of GVIA $iPLA_2$. Inhibitor *trans*-**9k** with a $X_I(50)$ value of 0.0000021 (IC_{50} 1 nM) is the most potent inhibitor of GVIA $iPLA_2$ ever reported in the literature, being a hundred times more potent than the fluoroketone inhibitor FKGK18. In addition, it is selective for GVIA $iPLA_2$, because it is 22,000 more potent for GVIA $iPLA_2$ than for GIVA $cPLA_2$. It reduces β-cell apoptosis induced by pro-inflammatory cytokines (IL-1β + IFNγ) in a concentration-dependent manner, suggesting that its use *in vivo* may be beneficial in reducing β-cell death leading to type 1 diabetes. This novel, highly potent and selective GVIA $iPLA_2$ inhibitor may be an excellent tool for the study of the role of the enzyme in cells and in animals and might help in developing novel medicinal agents.

EXPERIMENTAL SECTION

General.

Chromatographic purification of products was accomplished using Merck Silica Gel 60 (70–230 or 230–400 mesh). Thin-layer chromatography (TLC) was performed on Silica Gel 60 F254 aluminum plates. TLC spots were visualized with UV light and/or phosphomolybdic acid in EtOH. Melting points were determined using a Büchi 530 apparatus and were uncorrected. ^1H and ^{13}C NMR spectra were recorded on a Varian Mercury (200 MHz and 50 MHz, respectively) and a Bruker Avance III (600 MHz and 150 MHz, respectively) in $CDCl_3$. Chemical shifts are given in ppm, and coupling constants (*J*) in Hz. Peak multiplicities are described as follows: s, singlet, d, doublet, t, triplet and m, multiplet. Low resolution electron spray ionization (ESI) mass spectra were recorded on a Finnigan, Surveyor MSQ Plus spectrometer, while HRMS spectra were recorded on a Bruker Maxis Impact QTOF Spectrometer. Dichloromethane was dried by standard procedures and stored over molecular sieves. All other solvents and chemicals were reagent grade and used without further purification. The purity of all compounds subjected to biological tests was determined by analytical HPLC, and was found to be ≥95%. HPLC analyses were carried out on a Shimadzu LC-2010AHT system and an ODS Hypersil (250 × 4.6 mm, 5 μm) analytical column, using H_2O/acetonitrile 20/80 v/v, at a flow rate of 1.0 mL/min. HPLC analyses of *trans*-**9k** and *cis*-**9k** were carried out on a Agilent 1100 system and a Daicel Chiralcel OD-H (250 × 4.6 mm, 5 μm) using hexane/i-PrOH 95/5 v/v, at a flow rate of 1.0 mL/min.

Carboxylic acids **5a** and **5f** were commercially available. Carboxylic acids **5b**,[53] **5c**,[25] **5d**[25] and **5e**[53] have been described elsewhere and their analytical data are in accordance with literature. β-Hydroxy acids **8a-k** and β-lactones **9a-k** were obtained as mixtures of diastereomers. The diastereomeric ratio (d.r.) of the mixtures was determined by ^1H NMR spectroscopy.

General method for the synthesis of β-hydroxy acids (8a-k).

To a stirred solution of diisopropylamine (3 mmol) in anhydrous THF (2 mL), under argon at 0 °C, a solution of n-BuLi 1.6 M in hexane (3 mmol, 1.9 mL) was slowly added via syringe and the solution of LDA was stirred at 0 °C for 10 minutes. The carboxylic acid **7a-f** (1 mmol) in anhydrous THF (6 mL) was then added and the solution was stirred at 0 °C for 1 h. Then, aldehyde (1.3 mmol) in anhydrous THF (2 mL) was added and the solution was stirred at 0 °C for 1 h and at room temperature overnight. The solvent was removed under reduced pressure. The reaction mixture was acidified with HCl 1N to pH 2 and extracted with Et_2O (3× 20 mL). The organic layers were combined, washed with brine and dried. The solvent was removed and the product was purified by column chromatography eluting with a gradient of $CHCl_3$/MeOH 95/5 to 9/1.

3-Hydroxy-2-(3-phenylpropyl)nonanoic acid (8a).

Mixture of diastereomers (d.r. 6:4 *anti*:*syn*). Yield 51%; Oil; ^{1}H NMR (200 MHz, $CDCl_3$): δ 7.37–7.09 (m, 5H), 3.92–3.77 (m, 0.4H), 3.76–3.61 (m, 0.6H), 2.73–2.55 (m, 2H), 2.54–2.37 (m, 1H), 1.87–1.56 (m, 4H), 1.55–1.13 (m, 10H), 0.90 (t, *J* = 6.6 Hz, 3H); ^{13}C NMR (50 MHz, $CDCl_3$): δ 180.6, 141.8, 128.3, 128.2, 125.8, 72.2, 72.1, 50.9, 50.6, 35.7, 35.6, 35.2, 33.9, 31.7, 29.1, 29.0, 28.9, 28.7, 25.6, 22.6, 14.1; MS (ESI) m/z (%): 291.3 [$(M\text{-}H)^-$, 100]; HRMS: 315.1947 $(M+Na)^+$, (315.1931).

3-Hydroxy-2-(3-(naphthalen-2-yl)propyl)nonanoic acid (8b).

Mixture of diastereomers (d.r. 7:3 *anti*:*syn*). Yield 35%; Oil; ^{1}H NMR (200 MHz, $CDCl_3$): δ 7.86–7.65 (m, 3H), 7.55 (s, 1H), 7.48–7.21 (m, 3H), 3.93–3.75 (m, 0.3H), 3.74–3.57 (m, 0.7H), 2.85–2.65 (m, 2H), 2.56–2.29 (m, 1H), 1.91–1.56 (m, 4H), 1.56–1.03 (m, 10H), 0.84 (t, *J* = 6.4 Hz, 3H); ^{13}C NMR (50 MHz, $CDCl_3$): δ 180.7, 139.3, 133.5, 131.9, 127.8, 127.5, 127.4, 127.2, 126.3, 125.8, 125.1, 72.3, 72.2, 51.1, 50.9, 36.3, 35.8, 35.4, 34.0, 31.8, 29.2, 29.0, 28.9, 28.7, 25.6, 22.6, 14.1; MS (ESI) m/z (%): 341.3 [$(M\text{-}H)^-$, 100]; HRMS: 365.2090 $(M+Na)^+$, (365.2087).

2-(3-([1,1'-Biphenyl]-4-yl)propyl)-3-hydroxynonanoic acid (8c).

Mixture of diastereomers (d.r. 7:3 *anti*:*syn*). Yield 52%; Solid; mp 40–42 °C; ^{1}H NMR (200 MHz, $CDCl_3$): δ 7.60–7.21 (m, 9H), 3.95–3.83 (m, 0.3H), 3.79–3.63 (m, 0.7H), 2.75–2.60 (m, 3H), 1.88–1.60 (m, 4H), 1.53–1.13 (m, 10H), 0.88 (t, *J* = 6.0 Hz, 3H); ^{13}C NMR (50 MHz, $CDCl_3$): δ 180.6, 141.0, 138.8, 128.8, 128.7, 127.0, 126.9, 72.3, 72.2, 51.1, 50.9, 35.5, 35.3, 33.9, 33.9, 31.8, 29.5, 29.1, 29.0, 28.7, 25.6, 22.6, 14.1; MS (ESI) m/z (%): 367.2 [$(M\text{-}H)^-$, 100].

3-Hydroxy-2-(3-phenylpropyl)hexanoic acid (8d).

Mixture of diastereomers (d.r. 7:3 *anti*:*syn*). Yield 28%; Oil; ^{1}H NMR (200 MHz, $CDCl_3$): δ 7.37–7.07 (m, 5H), 3.94–3.80 (m, 0.3H), 3.79–3.67 (m, 0.7H), 2.72–2.57 (m, 2H), 2.57–2.42 (m, 1H), 1.89–1.56 (m, 4H), 1.56–1.30 (m, 4H), 0.93 (t, *J* = 6.2 Hz, 3H); ^{13}C NMR (50 MHz, $CDCl_3$): δ 180.6, 141.9, 128.3, 128.2, 125.8, 71.9, 71.8, 50.8, 50.7, 37.4, 36.1, 35.8, 35.6, 29.5, 29.0, 28.9, 26.3, 19.1, 18.8, 13.9; MS (ESI) m/z (%): 249.3 [$(M\text{-}H)^-$, 100]; HRMS: 273.1475 $(M+Na)^+$, (273.1461).

3-Hydroxy-2-(3-(naphthalen-2-yl)propyl)hexanoic acid (8e).

Mixture of diastereomers (d.r. 7:3 *anti*:*syn*). Yield 20%; Solid; mp 38–40 °C; ^{1}H NMR (200 MHz, $CDCl_3$): δ 7.90–7.67 (m, 3H), 7.60 (s, 1H), 7.50–7.19 (m, 3H), 3.94–3.80 (m, 0.3H), 3.80–3.62 (m, 0.7H), 2.78 (t, *J* = 6.0 Hz, 2H), 2.58–2.38 (m, 1H), 1.94–1.57 (m, 4H), 1.57–1.15 (m, 4H), 0.89 (t, *J* = 6.2 Hz, 3H); ^{13}C NMR (50 MHz, $CDCl_3$): δ 180.4, 139.3, 133.5, 131.9, 127.9, 127.5, 127.4, 127.1, 126.4, 125.9, 125.1, 71.9, 71.8, 51.0, 50.7, 37.4, 36.0, 35.9, 35.7, 29.3, 29.0, 28.9, 26.2, 19.1, 18.8, 13.9; MS (ESI) m/z (%): 299.3 [$(M-H)^-$, 100].

3-Hydroxy-2-(3-(4-methoxyphenyl)propyl)hexanoic acid (8f).

Mixture of diastereomers (d.r. 6:4 *anti*:*syn*). Yield 46%; Oil; ^{1}H NMR (200 MHz, $CDCl_3$): δ 7.06 (d, *J* = 8.0 Hz, 2H), 6.79 (d, *J* = 8.0 Hz, 2H), 3.95–3.80 (m, 0.4H), 3.79 (s, 3H), 3.78–3.59 (m, 0.6H), 2.56 (t, *J* = 6.8 Hz, 2H), 2.52–2.43 (m, 1H), 1.86–1.53 (m, 4H), 1.53–1.19 (m, 4H), 1.02–0.80 (m, 3H); ^{13}C NMR (50 MHz, $CDCl_3$): δ 180.3, 157.6, 134.0, 129.2, 113.7, 71.9. 71.8, 55.2, 50.9, 50.7, 37.4, 36.0, 34.8, 34.7, 29.7, 29.3, 28.9, 26.2, 19.1, 18.8, 13.9; MS (ESI) m/z (%): 279.2 [$(M-H)^-$, 100].

3-Hydroxy-4-methyl-2-(3-phenylpropyl)pentanoic acid (8g).

Mixture of diastereomers (d.r. 7:3 *anti*:*syn*). Yield 28%; Solid; mp 85–90 °C; ^{1}H NMR (200 MHz, $CDCl_3$): δ 7.46–7.03 (m, 5H), 3.64–3.45 (m, 0.3H), 3.45–3.25 (m, 0.7H), 2.72–2.44 (m, 2H and 0.7H), 2.43–2.27 (m, 0.3H), 1.89–1.40 (m, 5H), 1.05–0.72 (m, 6H); ^{13}C NMR (50 MHz, $CDCl_3$): δ 180.9, 180.7, 141.8, 128.3, 128.2, 125.8, 77.2, 48.3, 48.0, 35.8, 35.6, 31.8, 30.9, 29.5, 29.3, 29.0, 26.1, 19.6, 19.5, 17.5, 17.4; MS (ESI) m/z (%): 268.2 [$(M+NH_4^+)$, 100].

3-Hydroxy-2-(3-(naphthalen-2-yl)propyl)pentanoic acid (8h).

Mixture of diastereomers (d.r. 7:3 *anti*:*syn*). Yield 30%; Solid; mp 115–120 °C; ^{1}H NMR (200 MHz, $CDCl_3$): δ 7.83–7.70 (m, 3H), 7.60 (s, 1H), 7.48–7.28 (m, 3H), 3.78–3.68 (m, 0.3H), 3.60–3.53 (m, 0.7H), 2.75 (t, *J* = 6.0 Hz, 2H), 2.57–2.37 (m, 1H), 1.88–1.37 (m, 6H), 0.93 (t, *J* = 7.0 Hz, 3H); ^{13}C NMR (50 MHz, $CDCl_3$): δ 179.1, 139.5, 133.4, 131.8, 127.7, 127.4, 127.2, 127.1, 126.2, 125.7, 124.9, 73.7, 73.6, 51.1, 50.6, 35.8, 35.6, 29.3, 28.9, 28.8, 27.8, 10.3, 9.8; MS (ESI) m/z (%): 304.2 [$(M+NH_4^+)$, 100].

2-(1-Hydroxyethyl)-5-(naphthalen-2-yl)pentanoic acid (8i).

Mixture of diastereomers (d.r. 6:4 *anti*:*syn*). Yield 33%; Solid; mp 125–130 °C; ^{1}H NMR (200 MHz, $CDCl_3$): δ 7.86–7.70 (m, 3H), 7.60 (s, 1H), 7.50–7.25 (m, 3H), 4.12–3.99 (m, 0.4H), 3.99–3.86 (m, 0.6H), 2.79 (t, *J* = 6.6 Hz, 2H), 2.58–2.36 (m, 1H), 1.93–1.54 (m, 4H), 1.29–1.16 (m, 3H); ^{13}C NMR (50 MHz, $CDCl_3$): δ 180.0, 179.8, 139.2, 133.5, 132.0, 127.9, 127.6, 127.4, 127.1, 126.3, 125.9, 125.1, 68.3, 68.1, 52.6, 51.7, 35.9, 35.7, 29.3, 28.8, 26.7, 21.4, 20.0; MS (ESI) m/z (%): 290.4 [$(M+NH_4^+)$, 100].

3-Hydroxy-2-(4-(naphthalen-2-yl)butyl)hexanoic acid (8j).

Mixture of diastereomers (d.r. 6:4 *anti*:*syn*). Yield 20%; Solid; mp 36–38 °C; ^{1}H NMR (200 MHz, $CDCl_3$): δ 7.83–7.70 (m, 3H), 7.60 (s, 1H), 7.48–7.28 (m, 3H), 3.93–3.79 (m, 0.4H), 3.79–3.65 (m, 0.6H), 2.77 (t, *J* = 7.2 Hz, 2H), 2.53–2.39 (m, 1H), 1.85–1.59 (m, 4H), 1.58–

1.31 (m, 6H), 0.91 (t, *J* = 6.6 Hz, 3H); ^{13}C NMR (50 MHz, $CDCl_3$): *δ* 179.8, 139.8, 133.5, 131.9, 127.8, 127.6, 127.4, 127.3, 126.3, 125.8, 125.0, 71.8, 71.7, 50.7, 50.6, 37.6, 36.1, 35.8, 31.3, 31.1, 29.3, 27.4, 27.0, 26.5, 19.1, 18.9, 13.9; MS (ESI) m/z (%): 332.2 [(M +NH_4^+), 100].

3-Hydroxy-2-(4-phenylbutyl)hexanoic acid (8k).

Mixture of diastereomers (d.r. 7:3 *anti*:*syn*). Yield 68%; Solid; mp 38–40 °C; ^1H NMR (200 MHz, $CDCl_3$): *δ* 7.37–7.07 (m, 5H), 3.93–3.80 (m, 0.3H), 3.80–3.64 (m, 0.7H), 2.62 (t, *J* = 7.6 Hz, 2H), 2.53–2.37 (m, 1H), 1.85–1.55 (m, 4H), 1.55–1.27 (m, 6H), 0.94 (t, *J* = 7.0 Hz, 3H); ^{13}C NMR (50 MHz, $CDCl_3$): *δ* 180.5, 142.3, 128.3, 128.2, 125.7, 71.9, 71.8, 50.9, 50.7, 37.5, 36.1, 35.6, 31.4, 31.3, 29.2, 27.4, 26.9, 26.4, 19.1, 18.9, 13.9; MS (ESI) m/z (%): 282.2 [(M+NH_4^+), 100].

General method for the cyclization of β-hydroxy acids to β-lactones (9a-k).

To a stirred solution of β-hydroxy acid **8a-k** (1 mmol) in anhydrous pyridine (2 mL), under argon at 0 °C, p-toluenesulfonyl chloride (2 mmol) in anhydrous pyridine (1 mL) was added slowly via syringe. The solution was stirred at 0 °C for 1 h and kept at 4 °C for 3 days. Then, Et_2O was added and the organic layer was washed with 10% Na_2CO_3, HCl 1N to pH 2 and brine. The organic layer was dried and the solvent was removed in vacuo. The product was purified by column chromatography eluting with a gradient of petroleum ether (bp 40–60 °C) /AcOEt 95/5 to 9/1.

4-Hexyl-3-(3-phenylpropyl)oxetan-2-one (9a).

Mixture of diastereomers (d.r. 8:2 *trans*:*cis*).Yield 75%; Oil; ^1H NMR (200 MHz, $CDCl_3$): *δ* 7.35–7.11 (m, 5H), 4.58–4.44 (m, 0.2H), 4.27–4.13 (m, 0.8H), 3.68–3.53 (m, 0.2H), 3.26–3.11 (m, 0.8H), 2.65 (t, *J* = 6.8 Hz, 2H), 1.93–1.66 (m, 6H), 1.40–1.22 (m, 8H), 0.89 (t, *J* = 6.4 Hz, 3H); ^{13}C NMR (50 MHz, $CDCl_3$): *δ* 172.1, 171.4, 141.3, 128.4, 128.3, 126.0, 78.0, 75.6, 55.9, 52.4, 35.4, 34.4, 31.5, 30.1, 29.1, 28.8, 28.6, 27.3, 25.4, 24.9, 23.3, 22.5, 14.0; MS (ESI) m/z (%): 292.3 [(M+NH_4^+), 100]; HRMS: 297.1842 $(M+Na)^+$, (297.1825).

4-Hexyl-3-(3-(naphthalen-2-yl)propyl)oxetan-2-one (9b).

Mixture of diastereomers (d.r. 9:1 *trans*:*cis*).Yield 44%; Oil; ^1H NMR (200 MHz, $CDCl_3$): *δ* 7.87–7.72 (m, 3H), 7.60 (s, 1H), 7.52–7.23 (m, 3H), 4.60–4.41 (m, 0.1H), 4.27–4.10 (m, 0.9H), 3.69–3.55 (m, 0.1H), 3.27–3.10 (m, 0.9H), 2.82 (t, *J* = 7.0 Hz, 2H), 1.97–1.63 (m, 6H), 1.45–1.16 (m, 8H), 0.87 (t, *J* = 6.0 Hz, 3H); ^{13}C NMR (50 MHz, $CDCl_3$): *δ* 171.4, 138.8, 133.5, 132.0, 128.1, 127.6, 127.4, 127.0, 126.5, 126.0, 125.3, 78.0, 55.9, 35.6, 34.4, 31.6, 28.9, 28.5, 27.4, 25.0, 22.5, 14.0; MS (ESI) m/z (%): 342.2 [(M+NH_4^+), 100]; HRMS: 347.1986 $(M+Na)^+$, (347.1982).

3-(3-([1,1’-Biphenyl]-4-yl)propyl)-4-hexyloxetan-2-one (9c).

Mixture of diastereomers (d.r. 7:3 *trans*:*cis*).Yield 57%; Solid; mp 35–38 °C; ^1H NMR (200 MHz, $CDCl_3$): *δ* 7.64–7.16 (m, 9H), 4.61–4.44 (m, 0.3H), 4.27–4.15 (m, 0.7H), 3.71–3.55 (m, 0.3H), 3.28–3.12 (m, 0.7H), 2.70 (t, *J* = 6.8 Hz, 2H) 2.02–1.51 (m, 6H), 1.51–1.14 (m, 8H), 0.88 (t, *J* = 6.8 Hz, 3H); ^{13}C NMR (50 MHz, $CDCl_3$): *δ* 172.1, 171.4, 140.9, 140.4, 139.0, 128.8, 128.7, 127.2, 127.1, 127.0, 78.0, 75.6, 55.9, 52.5, 35.1, 34.4, 31.6, 30.1, 29.1, 28.9, 28.6, 27.4, 25.5, 25.0, 23.6, 22.5, 14.0; MS (ESI) m/z (%): 368.3 [(M+NH_4^+), 100]; HRMS: 373.2141 $(M+Na)^+$, (373.2138).

3-(3-Phenylpropyl)-4-propyloxetan-2-one (9d).

Mixture of diastereomers (d.r. 9:1 *trans*:*cis*). Yield 68%; Oil; ^{1}H NMR (200 MHz, $CDCl_3$): δ 7.40–7.10 (m, 5H), 4.60–4.45 (m, 0.1H), 4.28–4.13 (m, 0.9H), 3.68–3.54 (m, 0.1H), 3.26–3.10 (m, 0.9H), 2.66 (t, J = 7.0 Hz, 2H), 1.96–1.56 (m, 6H), 1.56–1.30 (m, 2H), 0.97 (t, J = 7.2 Hz, 3H); ^{13}C NMR (50 MHz, $CDCl_3$) δ 172.1, 171.4, 141.3, 128.4, 128.3, 126.0, 77.9, 75.4, 56.0, 52.5, 36.4, 35.5, 32.1, 29.2, 28.7, 27.4, 23.4, 18.9, 18.4, 13.8; MS (ESI) m/z (%): 250.1 [(M+NH_4^+), 100]; HRMS: 255.1358 $(M+Na)^+$, (255.1356).

***trans*-(±)-3-(3-Phenylpropyl)-4-propyloxetan-2-one (*trans*-9d).**

^{1}H NMR (200 MHz, $CDCl_3$): δ 7.36–7.10 (m, 5H), 4.28–4.13 (m, 1H), 3.26–3.10 (m, 1H), 2.66 (t, J = 7.0 Hz, 2H), 1.96–1.56 (m, 6H), 1.56–1.30 (m, 2H), 0.97 (t, J = 7.2 Hz, 3H); ^{13}C NMR (50 MHz, $CDCl_3$) δ 171.4, 141.3, 128.4, 128.3, 126.0, 77.9, 56.0, 36.4, 35.5, 28.7, 27.4, 18.4, 13.8.

***cis*-(±)-3-(3-Phenylpropyl)-4-propyloxetan-2-one (*cis*-9d).**

^{1}H NMR (200 MHz, $CDCl_3$): δ 7.36–7.10 (m, 5H), 4.60–4.45 (m, 1H), 3.68–3.54 (m, 1H), 2.66 (t, J = 7.0 Hz, 2H), 1.96–1.30 (m, 8H), 0.97 (t, J = 7.2 Hz, 3H); ^{13}C NMR (50 MHz, $CDCl_3$) δ 172.1, 141.3, 128.4, 128.3, 126.0, 75.4, 52.4, 35.4, 32.1, 29.1, 23.3, 18.8, 13.8.

3-(3-(Naphthalen-2-yl)propyl)-4-propyloxetan-2-one (9e).

Mixture of diastereomers (d.r. 8:2 *trans*:*cis*). Yield 66%; Oil; ^{1}H NMR (200 MHz, $CDCl_3$): δ 7.86–7.67 (m, 3H), 7.60 (s, 1H), 7.52–7.24 (m, 3H), 4.59–4.45 (m, 0.2H), 4.28–4.13 (m, 0.8H), 3.69–3.55 (m, 0.2H), 3.27–3.07 (m, 0.8H), 2.82 (t, J = 6.8 Hz, 2H), 1.96–1.62 (m, 6H), 1.51–1.25 (m, 2H), 0.95 (t, J = 6.8 Hz, 3H); ^{13}C NMR (50 MHz, $CDCl_3$): δ 172.1, 171.4, 138.8, 133.5, 132.0, 128.1, 127.6, 127.4, 127.0, 126.5, 126.0, 125.3, 77.8, 75.4, 56.0, 52.5, 36.4, 35.6, 32.1, 28.9, 28.5, 27.4, 23.4, 18.9, 18.4, 13.7; MS (ESI) m/z (%): 300.2 [(M +NH_4^+), 100]; HRMS: 305.1516 $(M+Na)^+$, (305.1512).

***trans*-(±)-3-(3-(Naphthalen-2-yl)propyl)-4-propyloxetan-2-one (*trans*-9e).**

^{1}H NMR (200 MHz, $CDCl_3$): δ 7.86–7.67 (m, 3H), 7.60 (s, 1H), 7.52–7.24 (m, 3H), 4.28–4.13 (m, 1H), 3.27–3.07 (m, 1H), 2.82 (t, J = 6.8 Hz, 2H), 1.96–1.62 (m, 6H), 1.51–1.25 (m, 2H), 0.95 (t, J = 6.8 Hz, 3H); ^{13}C NMR (50 MHz, $CDCl_3$): δ 171.4, 138.8, 133.5, 132.0, 128.1, 127.6, 127.4, 127.0, 126.5, 126.0, 125.3, 77.8, 56.0, 36.4, 35.6, 28.5, 27.4, 18.4, 13.8.

***cis*-(±)-3-(3-(Naphthalen-2-yl)propyl)-4-propyloxetan-2-one (*cis*-9e).**

^{1}H NMR (200 MHz, $CDCl_3$): δ 7.86–7.67 (m, 3H), 7.60 (s, 1H), 7.52–7.24 (m, 3H), 4.59–4.45 (m, 1H), 3.69–3.55 (m, 1H), 2.82 (t, J = 6.8 Hz, 2H), 1.96–1.25 (m, 8H), 0.95 (t, J = 6.8 Hz, 3H); ^{13}C NMR (50 MHz, $CDCl_3$): δ 172.1, 138.8, 133.5, 132.0, 128.1, 127.6, 127.4, 127.0, 126.5, 126.0, 125.3, 75.4, 52.5, 35.6, 32.1, 28.9, 23.4, 18.9, 13.8.

3-(3-(4-Methoxyphenyl)propyl)-4-propyloxetan-2-one (9f).

Mixture of diastereomers (d.r. 8:2 *trans*:*cis*). Yield 65%; Oil; ^{1}H NMR (200 MHz, $CDCl_3$): δ 7.09 (d, J = 8.4 Hz, 2H), 6.84 (d, J = 8.4 Hz, 2H), 4.62–4.47 (m, 0.2H), 4.28–4.14 (m, 0.8H), 3.79 (s, 3H), 3.68–3.51 (m, 0.2H), 3.27–3.08 (m, 0.8H), 2.60 (t, J = 7.0 Hz, 2H), 1.83–1.59 (m, 6H), 1.50–1.36 (m, 2H), 0.97 (t, J = 7.4 Hz, 3H); ^{13}C NMR (50 MHz, $CDCl_3$): δ 172.1, 171.4, 157.8, 133.3, 129.2, 113.8, 77.9, 75.4, 55.9, 55.2, 52.5, 36.4, 34.5, 32.1, 29.3, 28.9, 27.3, 23.3, 19.0, 18.4, 13.8; MS (ESI) m/z (%): 280.3 [(M+NH_4^+), 100]; HRMS: 285.1464 $(M+Na)^+$, (285.1461).

trans-(±)-3-(3-(4-Methoxyphenyl)propyl)-4-propyloxetan-2-one (*trans*-9f).

^{1}H NMR (200 MHz, $CDCl_3$): δ 7.09 (d, J = 8.4 Hz, 2H), 6.84 (d, J = 8.4 Hz, 2H), 4.28–4.14 (m, 1H), 3.79 (s, 3H), 3.27–3.08 (m, 1H), 2.60 (t, J = 7.0 Hz, 2H), 1.83–1.59 (m, 6H), 1.50–1.36 (m, 2H), 0.97 (t, J = 7.4 Hz, 3H); ^{13}C NMR (50 MHz, $CDCl_3$): δ 171.4, 157.8, 133.3, 129.2, 113.8, 77.9, 55.9, 55.2, 36.4, 34.5, 28.9, 27.3, 18.4, 13.7.

cis-(±)-3-(3-(4-Methoxyphenyl)propyl)-4-propyloxetan-2-one (*cis*-9f).

^{1}H NMR (200 MHz, $CDCl_3$): δ 7.09 (d, J = 8.4 Hz, 2H), 6.84 (d, J = 8.4 Hz, 2H), 4.62–4.47 (m, 1H), 3.79 (s, 3H), 3.68–3.51 (m, 1H), 2.60 (t, J = 7.0 Hz, 2H), 1.83–1.36 (m, 8H), 0.97 (t, J = 7.4 Hz, 3H); ^{13}C NMR (50 MHz, $CDCl_3$): δ 172.1, 157.8, 133.3, 129.2, 113.8, 75.4, 55.2, 52.5, 34.5, 32.1, 29.4, 23.3, 18.9, 13.8.

4-Isopropyl-3-(3-phenylpropyl)oxetan-2-one (9g).

Mixture of diastereomers (d.r. 7:3 *trans*:*cis*). Yield 36%; Oil; ^{1}H NMR (200 MHz, $CDCl_3$): δ 7.38–7.07 (m, 5H), 4.15–4.02 (m, 0.3H), 3.94–3.83 (m, 0.7H), 3.67–3.52 (m, 0.3H), 3.28–3.13 (m, 0.7H), 2.66 (t, J = 6.8 Hz, 2H), 2.12–1.57 (m, 5H), 1.03 (d, J = 6.6 Hz, 3H), 0.94 (d, J = 6.6 Hz, 2.1H), 0.88 (d, J = 6.6 Hz, 0.9H); ^{13}C NMR (50 MHz, $CDCl_3$): δ 172.1, 171.4, 141.3, 128.4, 128.3, 126.0, 82.7, 80.2, 53.9, 51.9, 35.5, 32.3, 28.9, 28.7, 27.7, 23.7, 19.0, 18.0, 17.0; MS (ESI) m/z (%): 250.2 [(M+NH_4^+), 100]; HRMS: 255.1357 $(M+Na)^+$, (255.1356).

4-Ethyl-3-(3-(naphthalen-2-yl)propyl)oxetan-2-one (9h).

Mixture of diastereomers (d.r. 7:3 *trans*:*cis*).Yield 53%; Oil; ^{1}H NMR (200 MHz, $CDCl_3$): δ 7.94–7.70 (m, 3H), 7.60 (s, 1H), 7.56–7.23 (m, 3H), 4.53–4.34 (m, 0.3H), 4.23–4.06 (m, 0.7H), 3.70–3.52 (m, 0.3H), 3.30–3.09 (m, 0.7H), 2.81 (t, J = 6.4 Hz, 2H), 2.07–1.58 (m, 6H), 1.09–0.91 (m, 3H); ^{13}C NMR (50 MHz, $CDCl_3$): δ 172.1, 171.3, 138.7, 133.4, 131.9, 128.0, 127.5, 127.3, 127.0, 126.4, 126.0, 125.2, 79.0, 76.8, 55.4, 52.3, 35.5, 28.9, 28.5, 27.4, 23.4, 23.3, 9.8, 9.1; MS (ESI) m/z (%): 286.3 [(M+NH_4^+), 100]; HRMS: 291.1356 $(M+Na)^+$, (291.1356).

4-Methyl-3-(3-(naphthalen-2-yl)propyl)oxetan-2-one (9i).

Mixture of diastereomers (d.r. 7:3 *trans*:*cis*). Yield 34%; Solid; mp 35–40 °C; ^{1}H NMR (200 MHz, $CDCl_3$): δ 7.86–7.71 (m, 3H), 7.60 (s, 1H), 7.48–7.28 (m, 3H), 4.81–4.63 (m, 0.4H), 4.45–4.30 (m, 0.6H), 3.71–3.52 (m, 0.4H), 3.27–3.10 (m, 0.6H), 2.82 (t, J = 6.6 Hz, 2H), 2.07–1.64 (m, 4H), 1.53 (d, J = 6.2 Hz, 2.1H*)*, 1.42 (d, J = 6.2 Hz, 0.9H); ^{13}C NMR (50

MHz, $CDCl_3$): δ 171.7, 171.0, 138.8, 138.7, 133.5, 132.0, 128.0, 127.6, 127.4, 127.0, 126.5, 126.0, 125.3, 125.2, 74.5, 71.6, 57.4, 52.6, 35.6, 28.7, 28.4, 27.2, 23.4, 20.3, 15.6; MS (ESI) m/z (%): 272.2 [(M+NH_4^+), 100]; HRMS: 277.1193 $(M+Na)^+$, (277.1199).

3-(4-(Naphthalen-2-yl)butyl)-4-propyloxetan-2-one (9j).

Mixture of diastereomers (d.r. 7:3 *trans*:*cis*).Yield 48%; Low melting point solid; ^{1}H NMR (200 MHz, $CDCl_3$): δ 7.87–7.69 (m, 3H), 7.60 (s, 1H), 7.52–7.23 (m, 3H), 4.59–4.42 (m, 0.3H), 4.27–4.10 (m, 0.7H), 3.66–3.50 (m, 0.3H), 3.23–3.05 (m, 0.7H), 2.79 (t, *J* = 7.2 Hz, 2H), 1.96–1.29 (m, 10H), 0.94 (t, *J* = 7.4 Hz, 3H); ^{13}C NMR (50 MHz, $CDCl_3$): δ 172.2, 171.6, 139.5, 133.5, 131.9, 127.9, 127.6, 127.3, 127.2, 126.3, 125.9, 125.1, 77.9, 75.4, 56.0, 52.5, 36.4, 35.6, 32.1, 31.0, 30.9, 27.7, 27.2, 26.5, 23.8, 18.8, 18.4, 13.7; MS (ESI) m/z (%): 314.4 [(M+NH_4^+), 100]; HRMS: 319.1675 $(M+Na)^+$, (319.1669).

trans-(±)-3-(4-(Naphthalen-2-yl)butyl)-4-propyloxetan-2-one (*trans*-9j).

^{1}H NMR (200 MHz, $CDCl_3$): δ 7.87–7.69 (m, 3H), 7.60 (s, 1H), 7.52–7.23 (m, 3H), 4.27–4.10 (m, 1H), 3.23–3.05 (m, 1H), 2.79 (t, *J* = 7.2 Hz, 2H), 1.96–1.54 (m, 6H), 1.54–1.29 (m, 4H), 0.94 (t, *J* = 7.4 Hz, 3H); ^{13}C NMR (50 MHz, $CDCl_3$): δ 171.6, 139.5, 133.5, 131.9, 127.9, 127.6, 127.3, 127.2, 126.3, 125.9, 125.1, 77.9, 56.0, 36.4, 35.6, 30.9, 27.7, 26.5, 18.4, 13.7.

cis-(±)-3-(4-(Naphthalen-2-yl)butyl)-4-propyloxetan-2-one (*cis*-9j).

^{1}H NMR (200 MHz, $CDCl_3$): δ 7.87–7.69 (m, 3H), 7.60 (s, 1H), 7.52–7.23 (m, 3H), 4.59–4.42 (m, 1H), 3.66–3.50 (m, 1H), 2.79 (t, *J* = 7.2 Hz, 2H), 1.96–1.29 (m, 10H), 0.94 (t, *J* = 7.4 Hz, 3H); ^{13}C NMR (50 MHz, $CDCl_3$): δ 172.2, 139.5, 133.5, 131.9, 127.9, 127.6, 127.3, 127.2, 126.3, 125.9, 125.1, 75.4, 52.5, 35.6, 32.1, 31.0, 27.2, 23.8, 18.8, 13.8.

3-(4-Phenylbutyl)-4-propyloxetan-2-one (9k).

Mixture of diastereomers (d.r. 7:3 *trans*:*cis*). Yield 68%; Oil; ^{1}H NMR (200 MHz, $CDCl_3$): δ 7.38–7.10 (m, 5H), 4.59–4.47 (m, 0.3H), 4.27–4.14 (m, 0.7H), 3.65–3.55 (m, 0.3H), 3.22–3.13 (m, 0.7H), 2.65 (t, *J* = 7.6 Hz, 2H), 1.96–1.54 (m, 6H), 1.54–1.30 (m, 4H), 0.97 (t, *J* = 7.2 Hz, 3H); ^{13}C NMR (50 MHz, $CDCl_3$): δ 172.2, 171.5, 142.0, 128.4, 128.3, 125.8, 77.9, 75.4, 55.9, 52.5, 36.4, 35.5, 32.1, 31.1, 31.0, 27.6, 27.1, 26.5, 23.7, 18.8, 18.3, 13.7; MS (ESI) m/z (%): 264.2 [(M+NH_4^+), 100]; HRMS: 269.1509 $(M+Na)^+$ (269.1512).

trans-(±)-3-(4-Phenylbutyl)-4-propyloxetan-2-one (*trans*-9k).

The mixture of diastereomers was separated by column chromatograhpy affording the *trans* diastereomer in 64% yield. Oil; ^{1}H NMR (600 MHz, $CDCl_3$): δ 7.32–7.29 (m, 2H), 7.23–7.18 (m, 3H), 4.23 (ddd, *J* = 7.4 Hz, 6.0 Hz, 4.0 Hz, 1H), 3.18 (ddd, *J* = 8.7 Hz, 6.7 Hz, 4.0 Hz, 1H), 2.65 (t, *J* = 7.6 Hz, 2H), 1.92–1.81 (m, 2H), 1.80–1.74 (m, 1H), 1.73–1.66 (m, 3H), 1.55–1.36 (m, 4H), 1.00 (t, *J* = 7.4 Hz, 3H); ^{13}C NMR (150 MHz, $CDCl_3$): δ 171.5, 142.0, 128.3, 125.8, 77.9, 56.0, 36.4, 35.5, 31.0, 27.7, 26.5, 18.4, 13.7.

cis-(±)-3-(4-Phenylbutyl)-4-propyloxetan-2-one (*cis*-9k).

The mixture of diastereomers was separated by column chromatograhpy affording the *cis* diastereomer in 8% yield. Oil; ^{1}H NMR (600 MHz, $CDCl_3$): δ 7.32–7.28 (m, 2H), 7.23–7.18 (m, 3H), 4.55 (ddd, J = 9.8 Hz, 6.4 Hz, 3.5 Hz, 1H), 3.61 (dt, J = 8.8 Hz, 6.7 Hz, 1H), 2.66 (t, J = 7.6 Hz, 2H), 1.87–1.80 (m, 1H), 1.78–1.54 (m, 7H), 1.49–1.39 (m, 2H), 1.01 (t, J = 7.3 Hz, 3H); ^{13}C NMR (150 MHz, $CDCl_3$): δ 172.2, 142.1, 128.3, 125.8, 75.4, 52.6, 35.5, 32.2, 31.1, 27.2, 23.8, 18.9, 13.8.

In vitro PLA_2 activity assay.

The activities of human recombinant GVIA $iPLA_2$, GIV $cPLA_2$ and GV $sPLA_2$ were determined using a previously described radioactivity-based group-specific mixed micelle assay.[41–43] The substrate was prepared using slightly different conditions for each enzyme to achieve optimum activity: (i) GIVA $cPLA_2$ mixed micelle substrate consisted of 400 µM Triton X-100, 95.3 µM PAPC, 1.7 µM arachidonyl-1-^{14}C PAPC, and 3 µM PIP_2 in a buffer containing 100 mM HEPES pH 7.5, 90 µM $CaCl_2$, 2 mM DTT, and 0.1 mg/ml BSA; (ii) GVIA $iPLA_2$ mixed micelle substrate consisted of 400 µM Triton X-100, 98.3 µM PAPC, and 1.7 µM arachidonyl-1-^{14}C PAPC in a buffer containing 100 mM HEPES pH 7.5, 2 mM ATP, and 4 mM DTT; and (iii) GV $sPLA_2$ mixed micelles substrate consisted of 400 µM Triton X-100, 98.3 µM PAPC, and 1.7 µM arachidonyl-1-^{14}C PAPC in a buffer containing 50 mM Tris-HCl pH 8.0, and 5 mM $CaCl_2$. The compounds were initially screened at 0.091 mole fraction (5 µL of 5 mM inhibitor in DMSO) in substrate (495 µL). $X_I(50)$ values were determined for compounds exhibiting greater than 95% inhibition. Inhibition plotting percentage of inhibition vs log (mole fraction) to calculate the reported $X_I(50)$ and its associated error.

For the *trans* and *cis* diastereomers of the most potent lactones, similar group specific PLA_2 assays were employed to determine the activity using a lipidomics-based mixed micelle assay as previously described.[44,45] The substrate for each enzyme consisted of 100 µM PAPC (except for GIVA $cPLA_2$ as noted), 400 µM of C12E8 surfactant, and 2.5 µM of 17:0 LPC internal standard. For GIVA $cPLA_2$, the total phospholipid concentration (100 µM) consisted of 97 µM PAPC and 3 µM of PI(4,5)P_2 which enhances the activity of the enzyme. A specific buffer was prepared to achieve optimum activity for each enzyme. The buffer for GIVA $cPLA_2$ contained 100 mM HEPES pH 7.5, 90 µM $CaCl_2$, and 2 mM DTT. For GVIA $iPLA_2$, the buffer consisted of 100 mM HEPES pH 7.5, 2 mM ATP, and 4 mM DTT. Finally, the buffer for GV $sPLA_2$ contained 50 mM Tris-HCl pH 8.0 and 5 mM $CaCl_2$. The enzymatic reaction was performed in a 96 well-plate using a Benchmark Scientific H5000-H MultiTherm heating shaker for 30 min at 40 °C. Each reaction was quenched with 120 µL of methanol/acetonitrile (80/20, v/v), and the samples were analyzed using a HPLC-MS system. A blank experiment, which did not contain enzyme, was also included for each substrate to determine the non-enzymatic hydrolysis product and to detect any changes in the intensity of the 17:0 LPC internal standard.

Docking calculations.

Enzyme structures were optimized using the PPW. The structures of the inhibitors were sketched using Maestro sketcher and they were optimized using LigPrep. Glide was used for the rigid-docking of the compounds into the enzyme active site. The grid required for the docking procedure was generated using a scaling factor of 1.0 and partial charge cutoff of 0.25, while *X*, *Y*, *Z* dimensions of the inner box were set to 12 Å. For the inhibitor docking a scaling factor of 0.8 and partial charge cutoff of 0.15 were used that allow complete flexibility of the structures. The poses were selected according to the binding mode and the XP GScore. The Glide Extra-Precision (XP) scoring function was used for the calculations.[54]

β-Cell apoptosis ± inhibitor trans-9k.

INS-1 cells were generated and cultured as previously described.[47] Briefly, the cells were cultured in RPMI 1640 medium, containing 11 mM glucose, 10% fetal calf serum, 10 mM HEPES buffer, 2 mM glutamine, 1 mM sodium pyruvate, 50 mM mercaptoethanol (BME), and 0.1% (w/v) each of penicillin and streptomycin in cell culture conditions (37 °C, 5% CO_2 /95% air), as described.[55] The cells were treated with vehicle (DMSO, 1 μL/mL) alone or with IL-1β (100 U/mL) + IFNγ (300 U/mL) for 16 h in the absence or presence of *trans*-**9k** (0.10–10 μM). The cells were then processed for apoptosis, by TUNEL analyses, as described.[47,50] Apoptotic cells (green fluorescence) and total number of cells, identifed by nuclear DAPI (blue) stain, in 6 fields on each slide were counted. Each slide represented one replicate (n=3–12). Percent apoptotic cells relative to total number of cells in each field was calculated and an average of the 6 fields/replicate was generated. The replicates were then averaged to generate means ± SEM for each condition and these are presented in Fig. 5.

Supplementary Material

Refer to Web version on PubMed Central for supplementary material.

ACKNOWLEDGEMENT

This research has been co-financed by the European Union (European Regional Development Fund-ERDF) and Greek national funds through the Operational Program “Competitiveness and Entrepreneurship” of the National Strategic Reference Framework (NSRF) - Research Funding Program: “Phospholipases A_2 inhibitors: Developing a drug pipeline for the treatment of inflammatory neurological disorders” (G.K.) and by NIH Grant RO1 GM20501–41 (E.A.D.) and NIH Grant RO1DK110292 (S. R.). C.D. would like to thank the National Scholarship Foundation (IKY) for a fellowship.

ABBREVIATIONS

ATP	adenosine triphosphate
BSA	bovine serum albumin
DAPI	4′,6-diamidino-2-phenylindole
DMF	N,N-dimethylformamide
DMSO	dimethyl sulfoxide
DTT	dithiothreitol
EtOAc	ethyl acetate

GIVA cPLA$_2$	Group IVA cytosolic phospholipase A$_2$
GVIA iPLA$_2$	Group VIA calcium-independent phospholipase A$_2$
GV sPLA$_2$	Group V secreted phospholipase A$_2$
HEPES	4-(2-hydroxyethyl)-1-piperazineethanesulfonic acid
IL-1β	interleukin 1β
INFγ	interferon γ
LDA	lithium diisopropylamide
PAPC	1-palmitoyl-2-arachidonylphosphatidylcholine
PIP$_2$	phosphatidyl inositol (4,5)-bisphosphate
PPW	protein preparation wizard
THF	tetrahydrofuran
Tris-HCl	tris(hydroxymethyl)aminomethane hydrochloride.

References

1. Dennis EA; Cao J; Hsu YH; Magrioti V; Kokotos G. Phospholipase A$_2$ enzymes: Physical structure, biological function, disease implication, chemical inhibition, and therapeutic intervention. Chem. Rev 2011, 111, 6130–6185. [PubMed: 21910409]
2. Winstead MV; Balsinde J; Dennis EA Calcium-independent phospholipase A$_2$: Structure and function. Biochim. Biophys. Acta 2000, 1488, 28–39. [PubMed: 11080674]
3. Cedars A; Jenkins CM; Mancuso DJ; Gross RWJ Calcium independent phospholipases in the heart: Mediators of cellular signaling, bioenergetics and ischemia-induced electrophysiologic dysfunction. J. Cardiovasc. Pharmacol 2009, 53, 277–289. [PubMed: 19390346]
4. Lei X; Barbour SE; Ramanadham S. Group VIA Ca2+-independent phospholipase A2 (iPLA2beta) and its role in beta-cell programmed cell death, Biochimie 2010, 92, 627–637. [PubMed: 20083151]
5. Ramanadham S; Ali T; Ashley JW; Bone RN; Hancock WD; Lei X. Calcium-independent phospholipases A$_2$ and their roles in biological processes and diseases. J. Lipid Res 2015, 56, 1643–1668. [PubMed: 26023050]
6. Hazen SL; Stuppy RJ; Gross RW Purification and characterization of canine myocardial cytosolic phospholipase A$_2$. A calcium-independent phospholipase with absolute f1–2 regiospecificity for diradyl glycerophospholipids. J. Biol. Chem 1990, 265, 10622–10630.
7. Ramanadham S; Wolf MJ; Jett PA; Gross RW; Turk J. Characterization of an ATP-stimulatable Ca^{2+}-independent phospholipase A$_2$ from clonal insulin-secreting HIT cells and rat pancreatic islets: A possible molecular component of the beta-cell fuel sensor. Biochemistry 1994, 33, 7442–7452. [PubMed: 8003509]
8. Ackermann EJ; Kempner ES; Dennis EA. Ca^{2+}-independent cytosolic phospholipase A$_2$ from macrophage-like P388D1 cells. Isolation and characterization. J. Biol. Chem 1994, 269, 9227–9233. [PubMed: 8132660]
9. Tang J; Kriz RW; Wolfman N; Shaffer M; Seehra J; Jones SS A novel cytosolic calcium independent phospholipase A$_2$ contains eight ankyrin motifs. J. Biol. Chem 1997, 272, 8567–8575. [PubMed: 9079687]
10. Balboa MA; Balsinde J; Jones SS; Dennis EA Identity between the Ca^{2+}-independent phospholipase A$_2$ enzymes from P388D1 macrophages and Chinese hamster ovary cells. J. Biol. Chem 1997, 272, 8576–8580. [PubMed: 9079688]

11. Ma Z; Ramanadham S; Kempe K; Chi XS; Ladenson J; Turk J. Pancreatic islets express a Ca^{2+}-independent phospholipase A_2 enzyme that contains a repeated structural motif homologous to the integral membrane protein binding domain of ankyrin. J. Biol. Chem 1997, 272, 11118–11127. [PubMed: 9111008]
12. Lio YC; Dennis EA Interfacial activation, lysophospholipase and transacylase activity of group VI Ca^{2+}-independent phospholipase A_2. Biochim. Biophys. Acta 1998, 1392, 320–332. [PubMed: 9630702]
13. Ong W-Y; Farooqui T; Kokotos G; Farooqui AA Synthetic and natural inhibitors of phospholipases A2: Their importance for understanding and treatment of neurological disorders. ACS Chem. Neurosci 2015, 6, 814–831. [PubMed: 25891385]
14. Kokotou MG; Limnios D; Nikolaou A; Psarra A; Kokotos G. Inhibitors of phospholipase A2 and their therapeutic potential: An update on patents (2012–2016). Expert Opin. Ther. Pat 2017, 27, 217–225. [PubMed: 27718763]
15. Magrioti V; Kokotos G. Phospholipase A2 inhibitors for the treatment of inflammatory diseases: A patent review (2010 – present). Expert Opin. Ther. Pat 2013, 23, 333–344. [PubMed: 23294257]
16. Leslie CC Cytosolic phospholipase A_2: Physiological function and role in disease. J. Lipid Res 2015, 56, 1386–1402. [PubMed: 25838312]
17. Murakami M; Taketomi Y; Miki Y; Sato H; Yamamoto K; Lambeau G. Emerging roles of secreted phospholipase A_2 enzymes: The 3rd edition. Biochimie 2014, 107 Pt A, 105–113. [PubMed: 25230085]
18. Ackermann EJ; Conde-Frieboes K; Dennis EA Inhibition of macrophage Ca^{2+}-independent phospholipase A_2 by bromoenol lactone and trifluoromethyl ketones. J. Biol. Chem 1995, 270, 445–450. [PubMed: 7814408]
19. Balsinde J; Dennis EA Bromoenol lactone inhibits magnesium-dependent phosphatidate phosphohydrolase and blocks triacylglycerol biosynthesis in mouse P388D_1 macrophages. J. Biol. Chem 1996, 271, 31937–31941.
20. Bone RN; Gai Y; Magrioti V; Kokotou MG; Ali T; Lei X; Tse HM; Kokotos G; Ramanadham S. Inhibition of Ca2+-independent phospholipase A2β (iPLA2β) ameliorates islet infiltration and incidence of diabetes in NOD mice. Diabetes 2015, 64, 541–554. [PubMed: 25213337]
21. Malhotra A; Edelman-Novemsky I; Xu Y; Plesken H; Ma J; Schlame M; Ren MC, Role of calcium-independent phospholipase A2 in the pathogenesis of Barth syndrome. PNAS 2009, 106, 2337–2341. [PubMed: 19164547]
22. Abi Nahed R; Martinez G; Escoffier J; Yassine S; Karaouzène T; Hograindleur JP; Turk J; Kokotos G; Ray PF; Bottari S; Lambeau G; Hennebicq S; Arnoult C. Progesterone-induced acrosome exocytosis requires sequential involvement of calcium-independent phospholipase A2β (iPLA2β) and Group X secreted phospholipase A2 (sPLA2). J. Biol. Chem 2016, 291, 3076–3089. [PubMed: 26655718]
23. Baskakis C; Magrioti V; Cotton N; Stephens D; Constantinou-Kokotou V; Dennis EA; Kokotos G. Synthesis of polyfluoro ketones for selective inhibition of human phospholipase A_2 enzymes. J. Med. Chem 2008, 51, 8027–8037. [PubMed: 19053783]
24. Kokotos G; Hsu Y-H; Burke JE; Baskakis C; Kokotos CG; Magrioti V; Dennis EA Potent and selective fluoroketone inhibitors of group VIA calcium-independent phospholipase A_2. J. Med. Chem 2010, 53, 3602–3610. [PubMed: 20369880]
25. Magrioti V; Nikolaou A; Smyrniotou A; Shah I; Constantinou-Kokotou V; Dennis EA; Kokotos G. New potent and selective polyfluoroalkyl ketone inhibitors of GVIA calcium-independent phospholipase A_2. Bioorg. Med. Chem 2013, 21, 5823–5829. [PubMed: 23916152]
26. Kalyvas A; Baskakis C; Magrioti V; Constantinou-Kokotou V; Stephens D; Lopez-Vales R; Lu JQ; Yong VW; Dennis EA; Kokotos G; David S. Differing roles for members of the phospholipase A_2 superfamily in experimental autoimmune encephalomyelitis. Brain 2009, 132, 1221–1235. [PubMed: 19218359]
27. Li J; Zhao Z; Antalis C; Zhao Z; Emerson R; Wei G; Zhang S; Zhang Z-Y; Xu Y. Combination therapy of an inhibitor of group VIA phospholipase A_2 with paclitaxel is highly effective in blocking ovarian cancer development. Am. J. Pathol 2011, 179, 452–461. [PubMed: 21703423]

28. Ali T; Kokotos G; Magrioti V; Bone RN; Mobley JA; Hancock W; Ramanadham S. Characterization of FKGK18 as inhibitor of Group VIA Ca2+-independent phospholipase A2 (iPLA2β): Candidate drug for preventing beta-cell apoptosis and diabetes. PLOS ONE 2013, 8: e71748.

29. Hsu YH; Bucher D; Cao J; Li S; Yang SW; Kokotos G; Woods VL Jr., McCammon JA; Dennis EA Fluoroketone inhibition of Ca^{2+}-independent phospholipase A_2 through binding pocket association defined by hydrogen/deuterium exchange and molecular dynamics, J. Am. Chem. Soc 2013, 135, 1330–1337. [PubMed: 23256506]

30. Bucher D; Hsu YH; Mouchlis VD; Dennis EA; McCammon JA Insertion of the Ca2+-independent phospholipase A2 into a phospholipid bilayer via coarse-grained and atomistic molecular dynamics simulations. PLoS Comput. Biol 2013, 9, e1003156.

31. Mouchlis VD; Bucher D; McCammon JA; Dennis EA Membranes serve as allosteric activators of phospholipase A2, enabling it to extract, bind, and hydrolyze phospholipid substrates. PNAS 2015, 112, E516eE525.

32. Mouchlis VD; Limnios D; Kokotou MG; Barbayianni E; Kokotos G; McCammon JA; Dennis EA Development of potent and selective inhibitors for group VIA calcium-independent phospholipase A_2 guided by molecular dynamics and structure-activity relationships. J. Med. Chem 2016, 59, 4403–4414. [PubMed: 27087127]

33. Weibel EK; Hadvary P; Hochuli E; Kupfer E; Lengsfeld H. Lipstatin, an inhibitor of pancreatic lipase, produced by Streptomyces Toxytricini. I. Producing organism, fermentation, isolation and biological activity. J. Antibiot 1987, 40, 1081–1085. [PubMed: 3680018]

34. Borgström B. Mode of action of tetrahydrolipstatin: a derivative of the naturally occurring lipase inhibitor lipstatin. Biochim. Biophys. Acta 1988, 962, 308–316. [PubMed: 3167082]

35. Bauer RA Covalent inhibitors in drug discovery: from accidental discoveries to avoided liabilities and designed therapies, Drug Discov. Today 2015, 20, 1061–1073. [PubMed: 26002380]

36. Kluge AF; Petter RC Acylating drugs: redesigning natural covalent inhibitors, Curr. Opin. Chem. Biol 2010, 14, 421–427. [PubMed: 20457000]

37. Black TH; DuBay WJ III A new synthesis of substituted spiro butyrolactones via dyotropic rearrangement. Tetrahedron Lett 1987, 28, 4787–4788.

38. Schmidt Y; Breit B. Enantioselective total synthesis and determination of absolute configuration of vittatalactone. Org. Lett 2009, 11, 4767–4769. [PubMed: 19791774]

39. Meier P; Broghammer F; Latendorf K; Rauhut G; Peters R. Cooperative Al(Salen)-pyridinium catalysts for the asymmetric synthesis of trans-configured β-lactones by [2+2]-cyclocondensation of acylbromides and aldehydes: Investigation of pyridinium substituent effects. Molecules 2012, 17, 7121–7150. [PubMed: 22692239]

40. Purohit VC; Richardson RD; Smith JW; Romo D. Practical, catalytic, asymmetric synthesis of β-lactones via a sequential ketene dimerization/hydrogenation process: Inhibitors of the thioesterase domain of fatty acid synthase. J. Org. Chem 2006, 71, 4549–4558. [PubMed: 16749788]

41. Kokotos G; Six DA; Loukas V; Smith T; Constantinou-Kokotou V; Hadjipavlou-Litina D; Kotsovolou S; Chiou A; Beltzner CC; Dennis EA Inhibition of group IVA cytosolic phospholipase A_2 by novel 2-oxoamides in vitro, in cells and in vivo. J. Med. Chem 2004, 47, 3615–3628. [PubMed: 15214789]

42. Stephens D; Barbayianni E; Constantinou-Kokotou V; Peristeraki A; Six DA; Cooper J; Harkewicz R; Deems RA; Dennis EA; Kokotos G. Differential inhibition of group IVA and group VIA phospholipases A_2 by 2-oxoamides. J. Med. Chem 2006, 49, 2821–2828. [PubMed: 16640343]

43. Six DA; Barbayianni E,; Loukas V; Constantinou-Kokotou V; Hadjipavlou-Litina D; Stephens D; Wong AC; Magrioti V; Moutevelis-Minakakis P; Baker SF; Dennis EA; Kokotos G. Structure-activity relationship of 2-oxoamide inhibition of group IVA cytosolic phospholipase A_2 and group V secreted phopholipase A_2. J. Med. Chem 2007, 50, 4222–4235. [PubMed: 17672443]

44. Mouchlis VD; Chen Y; McCammon JA; Dennis EA Membrane allostery and unique hydrophobic sites promote enzyme substrate specificity. J. Am. Chem. Soc 2018, 140, 3285–3291. [PubMed: 29342349]

45. Mouchlis VD; Armando A; Dennis EA Substrate specific inhibition constants for phospholipase A_2 acting on unique phospholipid substrates in mixed micelles and membranes using lipidomics. J. Med. Chem 2019, 62, DOI: 10.1021/acs.jmedchem.8b01568.

46. Dennis EA; Norris PC Eicosanoid storm in infection and inflammation. Nat. Rev. Immunol 2015, 15, 511–523. [PubMed: 26139350]

47. Ramanadham S; Hsu FF; Zhang S; Jin C; Bohrer A; Song H; Bao S; Ma Z; Turk J. Apoptosis of insulin-secreting cells induced by endoplasmic reticulum stress is amplified by overexpression of group VIA calcium-independent phospholipase A2 (iPLA2β) and suppressed by inhibition of iPLA2β. Biochemistry 2004, 43, 918–930. [PubMed: 14744135]

48. Lei X; Zhang S; Bohrer A; Bao S; Song H; Ramanadham S. The group VIA calcium-independent phospholipase A_2 participates in ER stress-induced INS-1 insulinoma cell apoptosis by promoting ceramide generation via hydrolysis of sphingomyelins by neutral sphingomyelinase. Biochemistry 2007, 46, 10170–10185

49 1. Lei X; Zhang S; Bohrer A; Ramanadham S. Calcium-independent phospholipase A2 (iPLA2β)-mediated ceramide generation plays a key role in the cross-talk between the endoplasmic reticulum (ER) and mitochondria during ER stress-induced insulin-secreting cell apoptosis. J. Biol. Chem 2008, 283, 34819–34832.

50. Lei X; Zhang S; Barbour SE; Bohrer A; Ford EL; Koizumi A; Papa FR; Ramanadham S. Spontaneous development of endoplasmic reticulum stress that can lead to diabetes mellitus is associated with higher calcium-independent phospholipase A_2 expression: A role for regulation by SREBP-1. J. Biol. Chem 2010, 285, 6693–6705. [PubMed: 20032468]

51. Lei X; Bone RN; Ali T; Wohltmann M; Gai Y; Goodwin KJ; Bohrer AE; Turk J; Ramanadham S. Genetic modulation of islet β-cell iPLA$_2$β expression provides evidence for its impact on β-cell apoptosis and autophagy. Islets 2013, 5, 29–44. [PubMed: 23411472]

52. Lei X; Zhang S; Bohrer A; Barbour SE; Ramanadham S. Role of calcium-independent phospholipase A_2β in human pancreatic islet β-cell apoptosis. Am. J. Physiol. Endocrinol. Metab 2012, 303, E1386–1395.

53. Huingen R; Rietz U. Mittlere Ringe, XIV. Darstellung und cyclisierung der ω-[naphthyl-(2)]-fettsäuren. Chem. Ber 1957, 90, 2768–2784.

54. Friesner RA; Murphy RB; Repasky MP; Frye LL; Greenwood JR; Halgren TA; Sanschagrin PC; Mainz DT Extra precision glide: Docking and scoring incorporating a model of hydrophobic enclosure for protein-ligand complexes. J. Med. Chem 2006, 49, 6177–6196. [PubMed: 17034125]

55. Ma Z; Zhang S; Turk J; Ramanadham S. Stimulation of insulin secretion and associated nuclear accumulation of iPLA(2)beta in INS-1 insulinoma cells. Am. J. Physiol. Endocrinol. Metab 2002, 282, E820–833. [PubMed: 11882502]

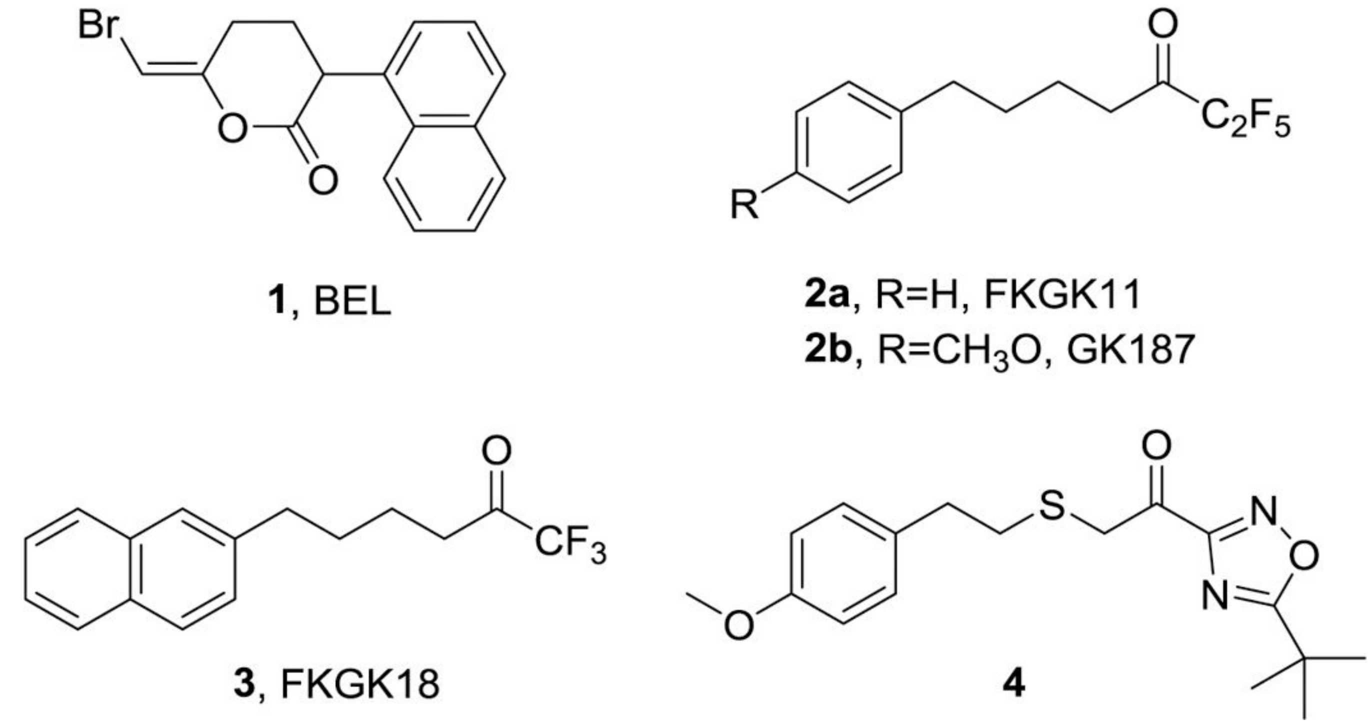

Figure 1.
Known inhibitors of GVIA $iPLA_2$.

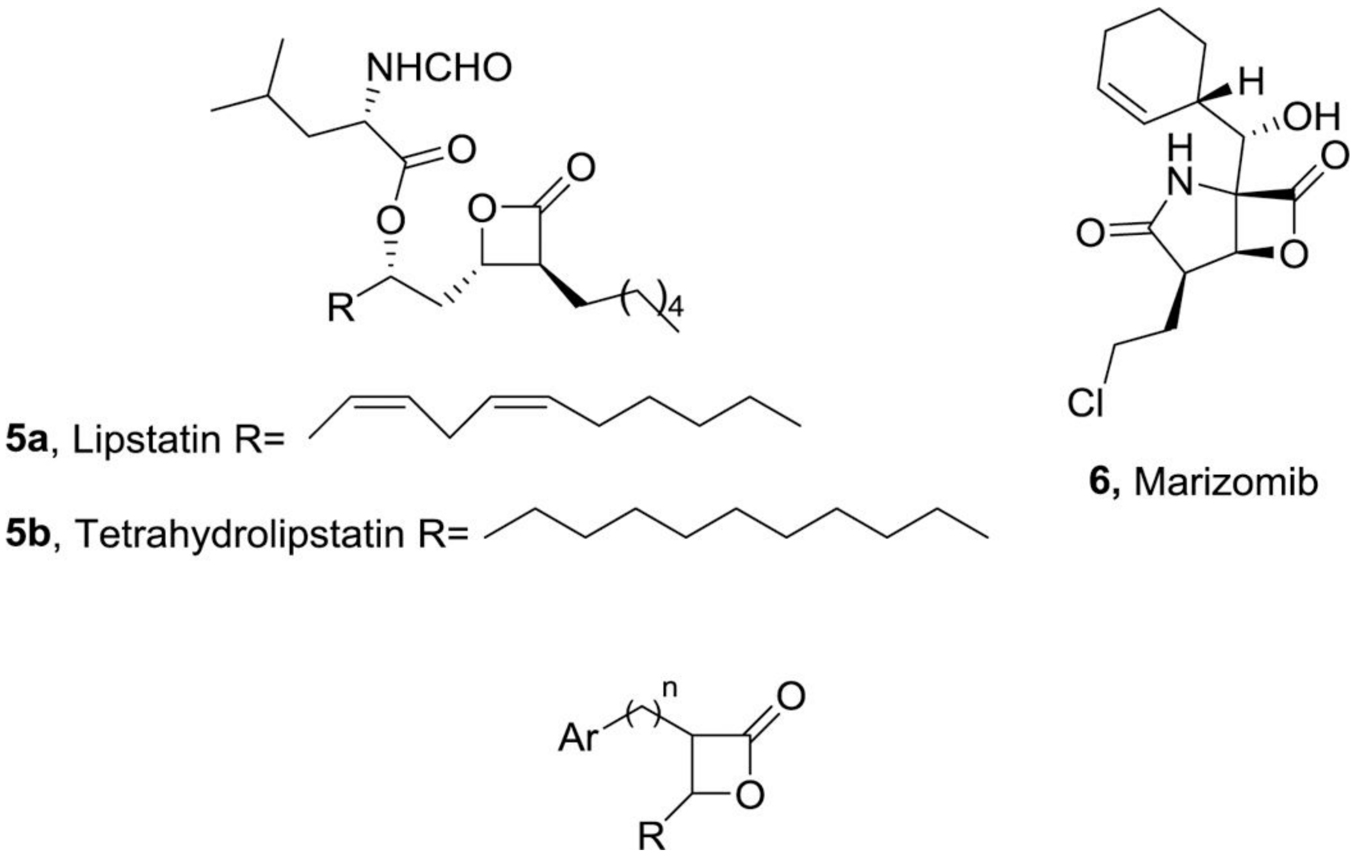

Figure 2.

Structures of lipstatin, tetrahydrolipstatin and marizomib and general structure of β-lactones designed in this study.

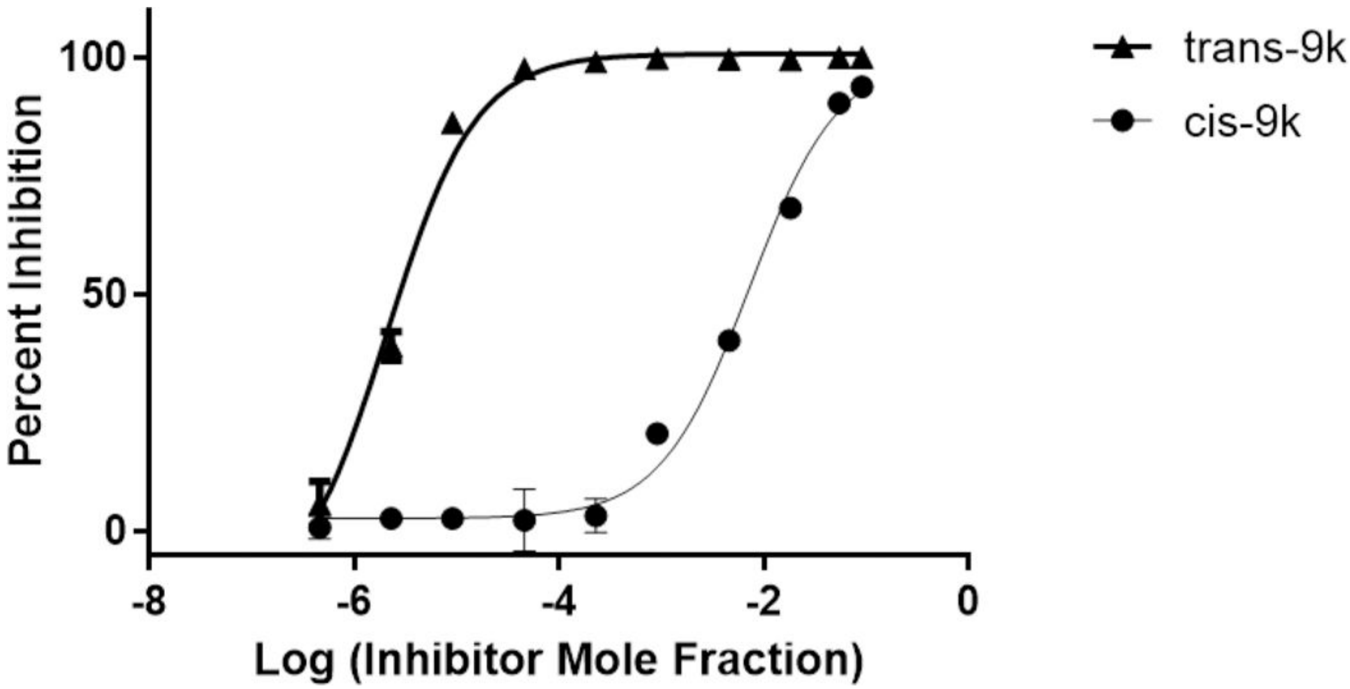

Figure 3.

Dose-response inhibition curves for GVIA iPLA$_2$ inhibitors *trans*-**9k** and *cis*-**9k**. The curves were generated using GraphPad Prism with a nonlinear regression targeted at symmetrical sigmoidal curves based on plots of % inhibition versus log(inhibitor concentration). The reported $X_I(50)$ values were calculated from the resultant plots.

Author Manuscript
Author Manuscript
Author Manuscript

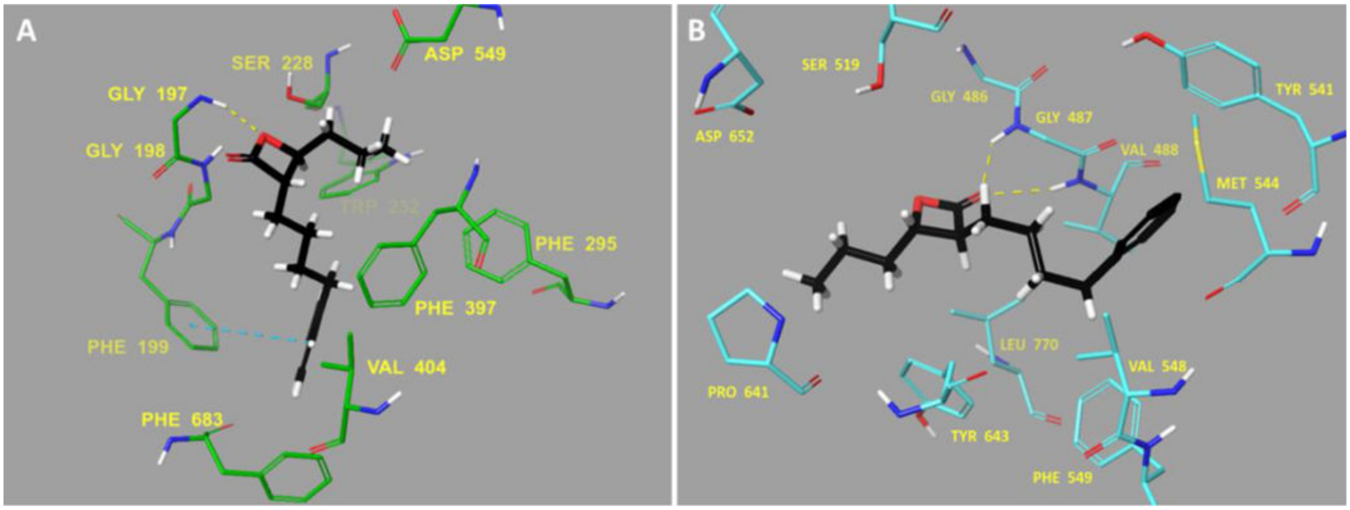

Figure 4.

Binding mode of *trans*-(*S*,*S*)-**9k** in the active site of (A) GIVA cPLA$_2$ (PDB ID: 1CJY) and (B) GVIA iPLA$_2$ (HM based on PDB ID: 1OXW).

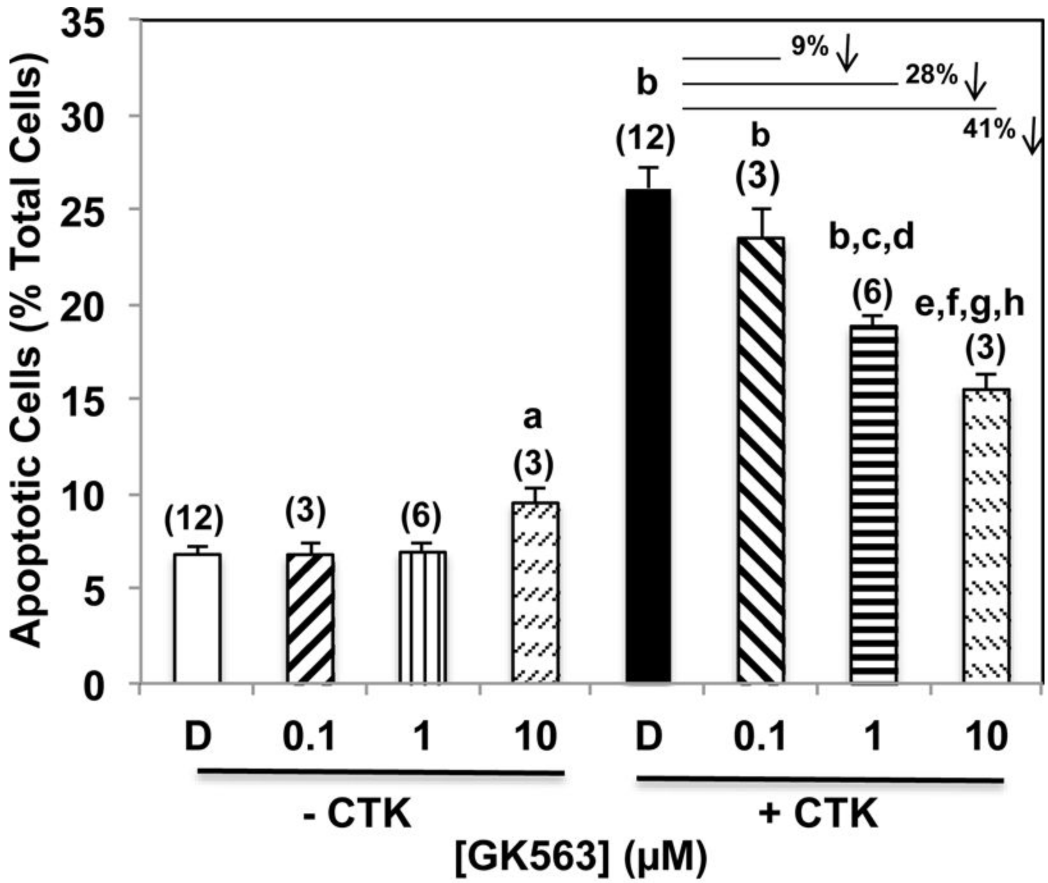

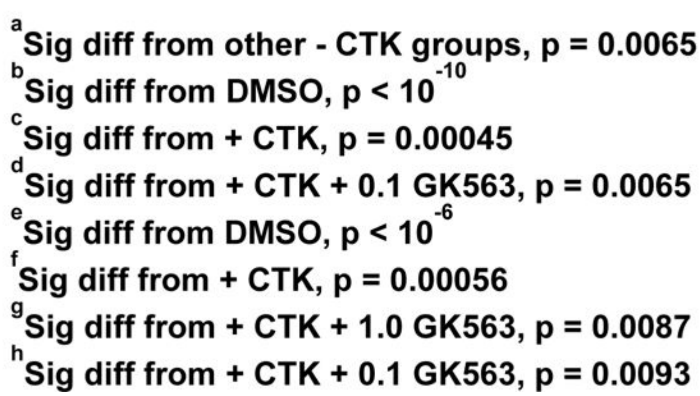

Figure 5.

INS-1 cell apoptosis ± *trans*-**9k**. INS-1 cells were treated with vehicle (DMSO) or cytokines (CTK, 100 U/mL IL-1β + 300 U/mL IFNγ) for 16 h in the absence or presence of *trans*-**9k** (0.10–10 μM). The cells were then processed for TUNEL analyses and the means ± SEM (n=3–12) of percent apoptotic cells relative to total number of cells are presented.

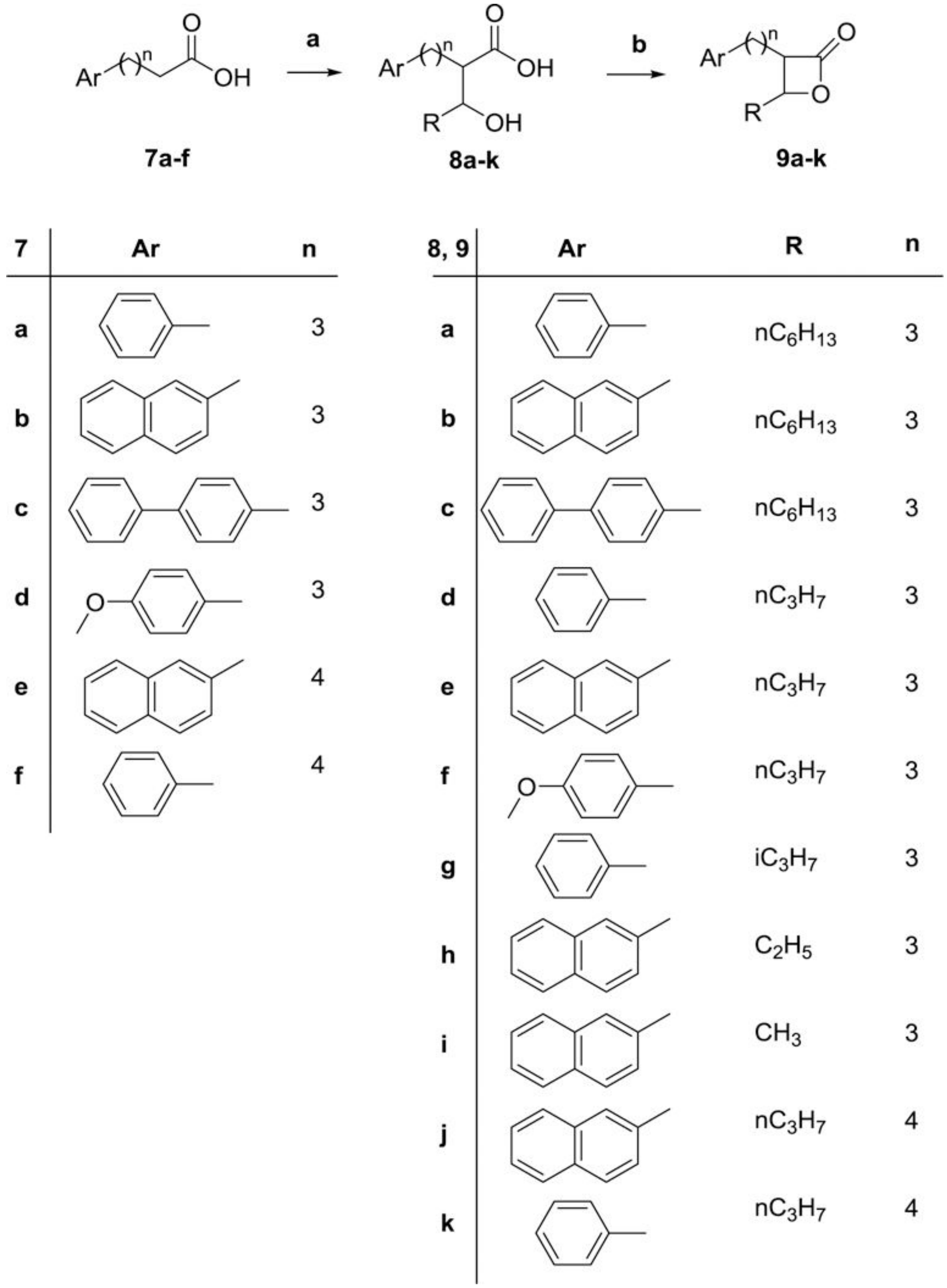

Scheme 1.

Reagents and conditions. (a) (i) LDA (produced in situ by $(i\text{-}Pr)_2NH$ and sol. n-BuLi 1.6 M/ hexane), dry THF, 0 ^{o}C, 1 h, (ii) solution of RCHO in dry THF, 0 ^{o}C, 1 h → r.t, o.n, (b) p-TsCl in dry pyridine, 0 ^{o}C, 1 h → 4 ^{o}C, 3 days.

Table 1.

In vitro potency and selectivity of β-lactones.

Entry	No	Structure	GVIA iPLA$_2$		GIVA cPLA$_2$		GV sPLA$_2$
			% Inhibition[a]	$X_I(50)$	% Inhibition[a]	$X_I(50)$	% Inhibition[a]
1	**9a**	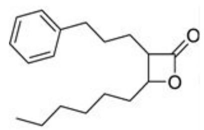	89 ± 2		91 ± 0.5		47 ± 8
2	**9b**	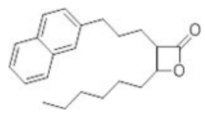	59 ± 7		54 ± 1		40 ± 8
3	**9c**	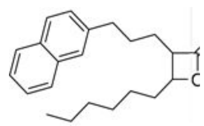	78 ± 4		58 ± 3		40 ± 6
4	**9d**	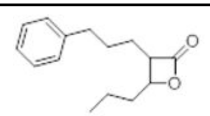	96 ± 1		81 ± 1		
5	***trans*-9d**	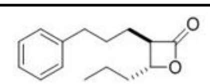	99 ± 0	0.00019 ± 0.00004	90 ± 1		25 ± 14
6	***cis*-9d**	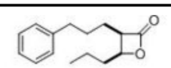	92 ± 1		97 ± 0	0.0019 ± 0.0004	N.D.[b]
7	**9e**	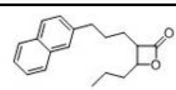	98 ± 2		77 ± 3		
8	***trans*-9e**	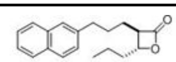	98 ± 0	0.00030 ± 0.00004	73 ± 3		30 ± 3

Entry	No	Structure	GVIA iPLA$_2$		GIVA cPLA$_2$		GV sPLA$_2$
			% Inhibition[a]	$X_I(50)$	% Inhibition[a]	$X_I(50)$	% Inhibition[a]
9	***cis*-9e**	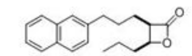	81 ± 1		89 ± 1		27 ± 10
10	**9f**	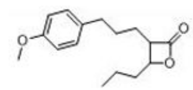	96 ± 1		76 ± 4		
11	***trans*-9f**	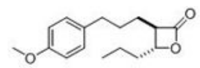	99 ± 1	0.00019 ± 0.00004	85 ± 2		26 ± 3
12	***cis*-9f**	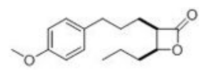	85 ± 1	0.038 ± 0.004	95 ± 1	0.00004 ± 0.00001	29 ± 1
13	**9g**	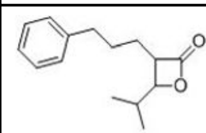	93 ± 0		85 ± 0.5		29 ± 2
14	**9h**	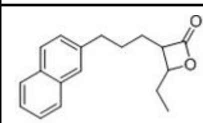	93 ± 0.0		85 ± 0.5		29 ± 2
15	**9i**	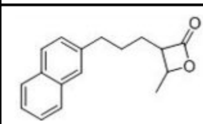	89 ± 0.0		85 ± 1		26 ± 9
16	**9j**	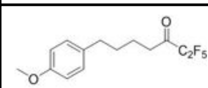	97 ± 3		71 ± 4		
17	***trans*-9j**	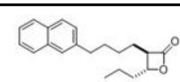	99 ± 0	0.00009 ± 0.00001	59 ± 2		29 ± 5

Entry	No	Structure	GVIA iPLA$_2$		GIVA cPLA$_2$		GV sPLA$_2$
			% Inhibition[a]	**$X_I(50)$**	**% Inhibition[a]**	**$X_I(50)$**	**% Inhibition[a]**
18	***cis*-9j**	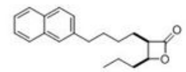	95 ± 1	0.0021 ± 0.0007	72 ± 6		N.D.
19	**9k**	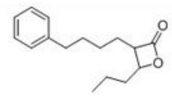	100 ± 0		84 ± 0		
20	***trans*-9k**	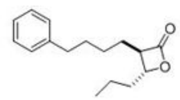	100 ± 0	0.0000021 ± 0.0000004	88 ± 3	0.042 ± 0.004	25 ± 8
21	***cis*-9k**	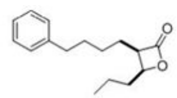	99 ± 0	0.007 ± 0.001	94 ± 1		34 ± 6
22	**2a**	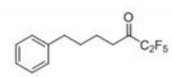	99 ± 0[24]	0.0014 ± 0.0001[24]	N.D.[24]		28 ± 1[24]
23	**2b**	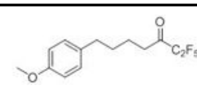	100[25]	0.0001 ± 0.0000[25]	N.D.[25]		33[25]
24	**3**	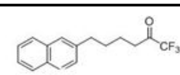	100 ± 0[24]	0.0002 ± 0.0000[24]	81 ± 1[24]		37 ± 8[24]
25	**4**	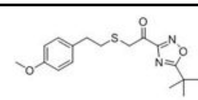	98 ± 0[32]	0.0057 ± 0.0012[32]	70 ± 2[32]		38 ± 4[32]

[a]% Inhibition at 0.091 mole fraction of each inhibitor.

[b]N.D. signifies compounds with less than 25% inhibition (or no detectable inhibition).